Vol. 1 June, 1955 No. 4

MINERALOGICAL JOURNAL

CONTENTS

Minerals of Bismuthinite-Stibnite Series with Special Reference to Horobetsuite from the Horobetsu Mine, Hokkaido, Japan ..... K. Hayase...189

X-ray Measurements of the Lattice Destruction and its Recovery on some Radioactive Minerals...T. Ueda and M. Korekawa...198

The Development of Pleochroic Haloes and the Alpha Radioactivity of the Nucleus Minerals ..... I. Hayase...213

Iron-rich Chlorite from Shōgasé, Kochi Prefecture, Japan ..... H. Shirozu...224

On the Structural Variations of some Japanese Kaolinites..... S. Iwai...233

On Inesite from Rendaiji.....S. Takasu...242

Short Communications

Recueil Mineralogique (III). (4) Riebeckite from Sepori in the Fukushin-san District, Korea. (5) Aegirine from Hoansan, in the Fukushin-san District, Korea..... J. Ito...250

The Mineralogical Society of Japan

Department of Geology and Mineralogy, Faculty of Science, Hokkaido University, Sapporo, Japan

MINERALOGICAL JOURNAL

published by

The Mineralogical Society of Japan

EDITORIAL BOARD

Zyunpei HARADA, *Hokkaido University;* Teiichi ITO, *University of Tokyo;* (Chief) Nobuo KATAYAMA, *University of Tokyo;* Keiichi OMORI, *Tohoku University;* Ryôiti KIRIYAMA, *University of Osaka;* Seitaro TSUBOI, *University of Tokyo;* Takeo WATANABE, *University of Tokyo;* Toyofumi YOSHIMURA, *Kyushu University.*

Instructions to Contributors

Manuscripts of articles should be submitted to the executive editor, Nobuo Katayama, at the College of General Education, University of Tokyo, Komaba, Meguro-ku, Tokyo. The manuscript should be type-written with double space lines, and not exceed 20 sheets of normal type-writing paper. References of literature should be in accordance with the forms used in the pages of this journal.

Plates and figures should be capable of reduction to not more than 10 by 15 centimetres. Line drawings should be in black India ink on white drawing board, tracing paper, or coordinate paper printed in blue. Photographs should be positive glossy prints.

Two referees chosen by the Editorial Board read the manuscript of article submitted before it is accepted for publication.

Thirty reprints without cover will be furnished to the author free of cost and without previous notice from him. Additional reprints will be furnished at cost when ordered.

The price of the journal to subscribers in Japan is 200 yen for a single copy (not including postage), and to subscribers in other countries $1.00 (including postage).

Printed in Japan

MINERALOGICAL JOURNAL VOL. 1, NO. 4, PP. 189–197, JUNE, 1955

MINERALS OF BISMUTHINITE-STIBNITE SERIES WITH SPECIAL REFERENCE TO HOROBETSUITE FROM THE HOROBETSU MINE, HOKKAIDO, JAPAN*

KITARO HAYASE

Institute of Mining, Faculty of Science and Engineering, Waseda University.

ABSTRACT

Horobetsuite occurs associated with free sulphur and iron sulphide minerals, in the sulphur deposit of Horobetsu Mine. The chemical formula of horobetsuite has been determined as $(Bi, Sb)_2S_3$. The molecular ratio of Bi_2S_3 to Sb_2S_3 varies between 9:11 and 13:7. The mineral is intermediate between bismuthinite and stibnite in lattice constant, specific gravity, optical behaviour and etching reaction. The data obtained reveal the mineral to be a new species belonging to the bismuthinite-stibnite series. A new mineral name, horobetsuite, is proposed for the mineral of the series which should have the molecular ratio of Bi_2S_3 to Sb_2S_3 between 7:3 and 3:7.

Introduction

The writer[1] once reported the results of the study of a Bi–Sb sulphide mineral that occurred at the Horobetsu mine, and suggested that it might represent a solid solution of bismuthinite and stibnite. The slight fluctuation observed of the molecular ratio of Bi_2S_3 to Sb_2S_3 has prompt us to a further study.

Occurrence of horobetsuite[1]

The Horobetsu mine in which horobetsuite occurs is located at Sobetsu Village, Usu County, in the vicinity of Muroran, Hokkaido, Japan. (Fig. 1)

---

* Read at the Annual Meeting of the Mineralogical Society of Japan held in Tokyo on June 4, 1954.

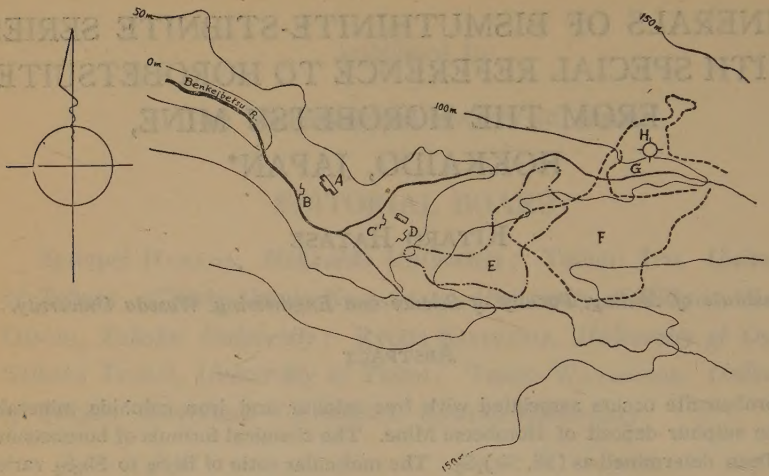

Fig. 1. Sulphur ore body of Horobetsu Mine. 1/20000

A: mining office.	B: adit of the 0 m.-level.
C: adit of the 25 m.-level.	D: adit of the 35 m.-level.
E: old ore body.	F: new ore body.
G: iron sulphide ore body.	H: locality of Horobetsuite.

The mother rocks of the deposit are altered andesitic tuff and agglomerate, and are impregnated with iron sulphide minerals and with a considerable amount of free sulphur.

Horobetsuite is found in the veinlets with many branches, which sometimes run along the bedding plane of the tuff, and sometimes penetrate into the iron sulphide ore. The average grade of Bi and Sb in the iron sulphide ore is respectively less than 1%. Other that iron sulphide minerals, free sulphur, opal and horobetsuite, no mineral is recognized to be present in the veinlets.

The succession of crystallization of these minerals is as follows: iron sulphide (pyrite and marcasite)→horobetsuite→free sulphur→opal.

Chemical composition and specific gravity of horobetsuite

Table 1 shows the results of the chemical analyses of horobetsuite and its specific gravity determined by means of a pycnometer.

Table 1. Chemical composition and specific gravity of horobetsuite.

Number of sample	Bi	Sb	S	Fe	Insol.	Total	Analyst	$G_4^{20°}$
No. 1	56.93%	21.49%	21.57%	tr.	tr.	99.99%	S. Ito[1]	——
No. 2	44.80	32.30	23.00	tr.	0.05%	100.15	S. Ito	5.449
No. 3*	51.84	17.20	24.15	5.20%	0.98	99.37	R. Sei[1]	——

* Iron sulphide could not be completely separated.

The ratio of Bi_2S_3 to Sb_2S_3 calculated varies from 9:11 to 13:7 as given in Table 2, in which are shown also the percentages of sulphur calculated from the molecular proportion and from the chemical analyses. The close agreement between the values indicates that the chemical composition of horobetsuite can be expressed as $(Bi, Sb)_2S_3$, unless the mineral is a mixture of bismuthinite and stibnite.

Table 2. Molecular proportion of Bi_2S_3 and Sb_2S_3 and percentage of sulphur for horobetsuite.

Number of sample	Bi_2S_3	Sb_2S_3	Percentage of sulphur	
			calculated from the mol. prop.	calculated from the analyses
No. 1	60.63%	39.37%	21.59%	21.57%
No. 2	44.62	55.38	23.07	23.00
No. 3	63.75	36.25	——	——

The specific gravity of the sample No. 2 was determined by means of a pycnometer as shown in Table 1. The observed value is intermediate between that of stibnite (4.63) and bismuthinite (6.78).

Etching reaction of horobetsuite[1)]

As shown in Table 3, horobetsuite lies between bismuthinite and stibnite in etching reaction.

Table 3. Etching reaction of bismuthinite, horobetsuite and stibnite[1)]

Reagent	Bismuthinite*	Horobetsuite	Stibnite**
1:1 HNO_3sol.	Stains brownish black	Same as the left	Same as the left
1:1 HCl sol.	Stains brown gradually	Do.	Do.
5% $HgCl_2$ sol.	None	Do.	Do.
20% $FeCl_3$ sol.	None	Do.	Do.
40% KOH sol.	None after a long time	Etching begins within 9~300 sec. Stains brown	Etched instantly and becomes rough
20% KCN sol.	None	Etching begins within 35~85 sec. Stains brown	Etching begins within 30~40 sec.

* From the Ashiyasu mine, Yamanashi Prefecture.
** From the Ichinokawa mine, Ehime Prefecture.

When horobetsuite is etched with KOH or KCN solution, it shows a beautiful zonal structure due to various etching speeds in each zone. (Plate I, Fig. 2)

From the results of the microchemical test and the spot test, it was indicated that there was no remarkable difference of the content of Bi and Sb between the zones with higher and lower etching speed.

Crystal habit of horobetsuite

The crystal of horobetsuite is of a prismatic habit with striations parallel to the prism zone. It is usually idiomorphic, and the dimension of a single crystal is 1.0~7.0 mm. in length and 0.2~2.0 mm. in diameter. (Plate I, Fig. 3)

It is very difficult to separate horobetsuite crystals from other ore minerals as it is enclosed in them. No optical goniometry was tried.

Optical properties of horobetsuite

Horobetsuite is lead-gray in colour and black in streak.

Under the microscope, as shown in Table 4 and Plate I, Figs. 4 and 5, horobetsuite seems to lie between bismuthinite and stibnite in optical properties.

Table 4. Optical properties of bismuthinite, horobetsuite and stibnite.

Optical property	Bismuthinite*	Horobetsuite	Stibnite**
Reflexion colour	White	White	White
Pleochroism	Pale pink~pale blue	Not distinctive	Not distinctive
Do. in oil	Increases distinctness	Very pale brown ~pale blue	Slightly recognized
Polarization colour	Pale pink~pale gray~dark brown	Pale yellow~gray ~dark brown	Pale brown~ dark brown
Do. in oil	More distinctive	More distinctive	More distinctive
Extinction	Straight Extinction (4 times per rot.)	Same as the left	Same as the left
Hardness	Ca. B.	Ca. B.	Ca. B

* From the Ashiyasu mine, Yamanashi Prefecture.

** From the Ichinokawa mine, Ehime prefecture.

X-ray diffraction patterns

Powdered crystals of horobetsuite was examined by means of a Philips X-ray spectrometer under the operating conditions as follows:

X-ray radiation: Cu $K\alpha$, 35 kV., 15 mA.,
filter: 0.0006″ nickel foil,
scanning speed: 2°/min..

In Table 5 there are shown the X-ray powder patterns of stibnite, horobetsuite and bismuthinite.

For the X-ray examination the sample No. 2 in Table 1 was used.

The lattice constants of horobetsuite were calculated from the *d*-values of (320), (211) and (221) on the basis of the standard rock

Table 5. X-ray powder data.

Stibnite			Horobetsuite				Bismuthinite		
				d					
I	*d*	(*hkl*)	*I*	observed	calculated	(*hkl*)	*I*	*d*	(*hkl*)
67	5.63Å	(200)	36	5.63Å	5.62Å	(200)	30	5.67Å	(200)
49	5.04	(120)	26	5.05	5.04	(120)	23	5.04	(120)
18	3.97	(220)	25	3.97	3.98	(220)	32	3.97	(220)
100	3.55	(310)	100	3.56	3.55	(310)	100	3.55	(310)
—	—	—	—	—	—	—	6	3.34	?
—	—	—	—	—	—	—	4	3.25	(201)?
27	3.11	(320)	25	3.11	3.12	(320)**	43	3.11	{(320) (211)}
23	3.04	(211)	29	3.08	3.08	(211)**	—	—	—
25	2.75	(221)	23	2.78	2.78	(221)	23	2.80	(221)
11	2.67	(031)	—	—	—	—	—	—	—
—	—	—	9	2.70	2.72	(410)	10	2.71	(410)
4	2.60	(311)	5*	2.63	2.63	(311)	8	2.64	(311)
54	2.51	(420)	49	2.51	2.51	(420)	34	2.52	(420)
7	2.41	(321)	7	2.44	2.44	(321)	5	2.45	(321)
16	2.27	(401)	15	2.29	2.28	(401)	8	2.30	(401)
9	2.24	(340)?	—	—	—	—	—	—	—
12	2.23	(141)	23	2.24	2.24	(141)	19	2.25	(141)
24	2.09	(421)	—	—	—	—	4*	2.12	(421)
—	—	—	18	2.09	2.09	(520)	4*	2.09	(520)
6	1.98	(440)	—	—	—	—	—	—	—
23	1.93	(431)?	—	—	—	—	—	—	—
15	1.92	(530)?	6	1.98	—	?	—	—	—
12	1.91	(002)	27	1.94	1.95	{(002) (431)}	7	1.98	(002)
—	—	—	—	—	—	—	20	1.95	(431)
18	1.88	?	—	—	—	—	—	—	—
—	—	—	15	1.92	—	?	—	—	—
10	1.85	(112)	24	1.88	1.89	(112)	—	—	—
—	—	—	6*	1.86	—	?	—	—	—
—	—	—	6*	1.84	1.84	(022)	15	1.88	(022)
3*	1.78	(212)	4*	1.78	1.81	(212)	7	1.85	(212)
3*	1.75	?	—	—	—	—	—	—	—
12	1.72	(222)	10	1.73	1.75	(222)	3*	1.78	(222)?
29	1.68	(312)	7	1.71	1.71	(312)	12	1.73	(312)

*: broad peak, **: doublet.

salt mixed with the sample. The results are shown in Table 6 compared with the lattice constants of bismuthinite and stibnite.

Table 6. Lattice constants.

	a_0	b_0	c_0
Bismuthinite*	11.13±0.02	11.27±0.02	3.97±0.01
Horobetsuite	11.24	11.28	3.90
Stibnite*	11.20±0.02	11.28±0.02	3.83±0.01

* After Dana's System of Mineralogy 7th ed, Vol. 1, (1946).

We read from the Table that bismuthinite has c_0 larger than horobetsuite which has again larger c_0 than stibnite, while the b_0 lengths of them all are nearly identical. As a consequence, the spacings of (320) of the three minerals should be scarcely different from each other against the distinct divergency of those of (211). (Fig. 6)

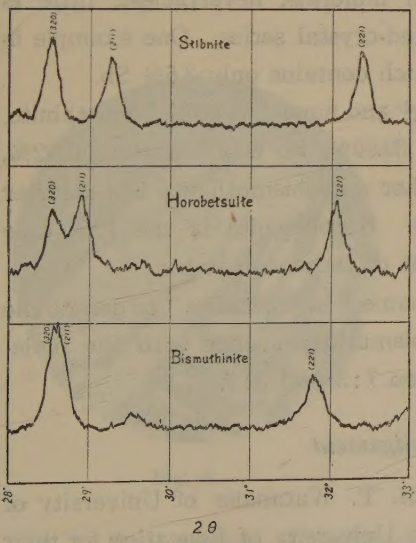

Fig. 6. The chart of X-ray spectrometer for stibnite horobetsuite and bismuthinite.
Ratemeter: 4-1-8, scanning speed: ¼°/min.

As is obvious in Fig. 6, in stibnite the peak (320) is separate from (211), while in bismuthinite both peaks (320) and (211) coincide. The spacings of (211) of bismuthinite and stibnite are different from each other.

As for the spacings of (221) and (211) of horobetsuite, they take intermediate values between those of bismuthinite

and stibnite, while all spacings of (320) of the three minerals take almost the same values as shown in Table 5.

Examinations by the lower scanning speed (¼°/min) for the three minerals fully verified the aforesaid relationship as shown in Fig. 6.

Notwithstanding the distinct zonal structure, neither double nor broad peak is found in the patterns of horobetsuite compared with those of bismuthinite and stibnite.

In considering these facts, the writer infers that horobetsuite is not a mixture of but a soild solution of bismuthinite and stibnite, and that as far as we witnessed the ratio of Bi_2S_3 to Sb_2S_3 in a single crystal has only a limited range.

Relation between horobetsuite and the related minerals

Y. Takahashi[4] reported that Bi_2S_3 and Sb_2S_3 make a perfect mixed-crystal series. Among the natural minerals, nevertheless, little is known about the Bi_2S_3–Sb_2S_3 mixed-crystal series. One example is the bismuthinite from Tazna[3], which contains only 3.5% Sb.

Another was reported by Koenig[2] and named as stibiobismuthinite, with the chemical composition Bi 69.90%, Sb 8.12% and S 21.92%, but it is not yet determined whether stibiobismuthinite is a member of the stibnite-bismuthinite series. Horobetsuite is the first case containing nearly the same amount of the end member.

Hence, the writer propose the name "horobetsuite" to denote the mineral belonging to the stibnite-bismuthinite series with the molecular ratio of Sb_2S_3 to Bi_2S_3 between 7:3 and 3:7.

Acknowledgement

The writer wishes to thank Prof. T. Watanabe of University of Tokyo and Prof. T. Sudo of Tokyo University of Education for their helpful suggestions, and Mr. K. Sakurai for his offering the valuable sample of stibiobismuthinite. He is also indebted to the Institute of Geology, University of Tokyo, for permission of using the Norelco X-ray spectrometer.

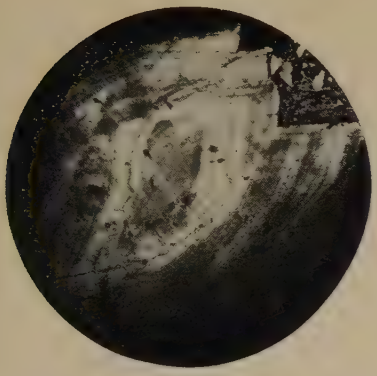

Fig. 2.

Fig. 3.

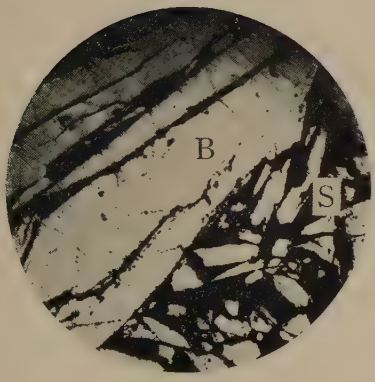

Fig. 4.

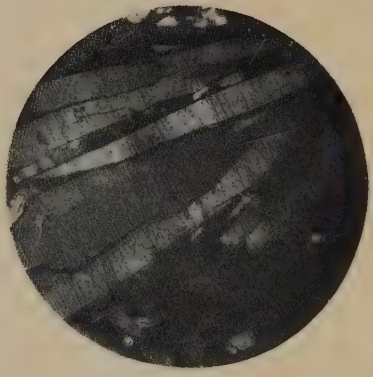

Fig. 5.

Fig. 2. Zonal structure of horobetsuite etched with KCN solution. (×56)
Fig. 3. Crystals of horobetsuite isolated by treating the ore with CS_2. (×11)
Fig. 4. Photomicrographs of horobetsuite without analyzer. (×56)
B: horobetsuite. S: free sulphur.
Fig. 5. ditto, with analyzer. (×56)

REFERENCES

1) Hayase, K.: Mining Geology, **2**, 177 (1952). (In Japanese)
2) Palache C., H., H. Berman and C. Frondel: Dana's System of Mineralogy, Vol. 1, 278 (1946).
3) Peacock, M. A.: Z. X., **86**, 203 (1933).
4) Takahashi, Y.: Mem. Coll. Sci. Kyoto Univ., **4**, 47 (1920).

Manuscript received September 1, 1954.

MINERALOGICAL JOURNAL, VOL. 1, NO. 4, PP. 198-212, JUNE, 1955

X-RAY MEASUREMENTS OF THE LATTICE DESTRUCTION AND ITS RECOVERY ON SOME RADIOACTIVE MINERALS*

TATEO UEDA and MASAAKI KOREKAWA

Institute of Geology and Mineralogy, Faculty of Science, University of Kyoto

ABSTRACT

X-ray measurements were carried out in order to study the spontaneous radiation effects of allanite, gadolinite and monazite on their structures. It was found that the first two gave the experimental evidences of either expansions from or destruction of their normal lattice structures, while the last one showed lattice expansion only. Heat treatments of these minerals in the vacuum caused them to recover their normal lattice states.

Introduction

It has long been assumed by mineralogists that the bombardment of alpha-particles, which are liberated in radioactive minerals on disintegration, on their constituent atoms and recoiling of parent atoms are the cause of the metamict states often observed with these minerals. It is also a well-known fact, however, that there are certain minerals such as monazite and autunite, which are radioactive but not found in a metamict state; the fact suggests that there must be some other factors which play important roles in metamictization of radioactive minerals. In fact, several research workers[3)5)6)10)] have hitherto given some considerations on this problem and among them Pellas[7)8)] reached an important conclusion that the condition prerequisite to metamictization was the existence

* A preliminary report of this work was read at the meeting of the Mineralogical Society of Japan held in Fukuoka on October 31, 1954.

of partially directed bonds in the structures. Then, Stech[9], who studied changes in crystal structures caused by the bombardment of alpha-particles, observed no structure change occurred in crystals with strong bonds and with high degrees of space utilization, and strong columnar ionization by the particles was necessary for structure changes. Recently, Hurley and Fairbairn[2] on their study on zircon found that the lattice expanded as the metamictization proceeded. The present authors[12] also observed the same fact on their study on allanite, gadolinite and monazite.

The following report is to deal with this problem of lattice expansion in some metamict minerals with X-ray spectrometric data recently obtained.

Experimental

Specimens used in the present work were as follows:

Mineral	Locality			
Allanite	Daimonji-yama,	Kyoto	Prefecture,	Japan.
	Mie-mura,	Kyoto	Prefecture,	
	Ôyama-mura,	Toyama	Prefecture,	
	Kido-mura,	Shiga	Prefecture,	
	Hagata-mura,	Ehime	Prefecture,	
	Nogizawa-mura,	Fukushima	Prefecture,	
	Kojima-mura,	Fukushima	Prefecture,	
	Anak-ub,	Howangheto,		Korea.
	Hakson-myon,	Hamkyonpekto,		
	Santaikou,			South Manchuria.
	Tafangshen,			
	Tungwenchungtan,			North China.
Gadolinite	Arendal,			Norway.
Monazite	Kôbe-mura,	Kyoto	Prefecture,	Japan.
	Harimichi-mura,	Fukushima	Prefecture,	
	Ishikawa-machi,	Fukushima	Prefecture,	

The Geiger counter X-ray spectrometer of North American Philips Co. was employed throughout the experiments with filtered Cu-$K\alpha$ radiation and powder diffraction data were obtained under the following conditions: scan speed, 1° per minute; scaler, 4 or 8; time constant, 8, and chart speed, $\frac{1}{2}$ inch per minute. Having been calibrated with the diffraction lines of silicon, the spacings were calculated by the method of least squares. The peaks whose glancing angles were smaller than 25.65°(2θ), that is, whose spacings were larger than 3.471Å, were not adopted in the present case, for no silicon diffraction peak was observable in this range.

Measurements were also carried out with heat-treated specimens. The specimens were heated in a rheostat-controlled furnace for two hours[11] at about 400°C and 800°C under the pressure of 10^{-4} mm Hg in closed silica tubes as well as under the atmospheric pressure.

Description of the experimental results

Allanite

a) Unheated specimens: The diffraction patterns of unheated specimens are shown in Fig. 1. As will be seen in this figure, the diffraction patterns widely vary from each other in sharpness, and diffuse ones generally give asymmetric peaks. The diffuseness of these patterns may reasonably be taken as a measure of the progress of metamictization of the respective specimens.

Spacings calculated from the peaks are given in Table 1, in which the numbers in the bottom row denote the order of sharpness of the patterns estimated by inspection. It is to be noticed here that as a general tendency the spacings become larger as the metamictization proceeds, though there are some deviations from this rule as seen, for example, between the specimen from Daimonji-yama and that from Ôyama-mura. Discussions on this point as well as on the asymmetry of peaks were given in the previous paper by the present authors[12]. The indices given in the first column in the table were derived from the lattice constants determined by Ueda[13].

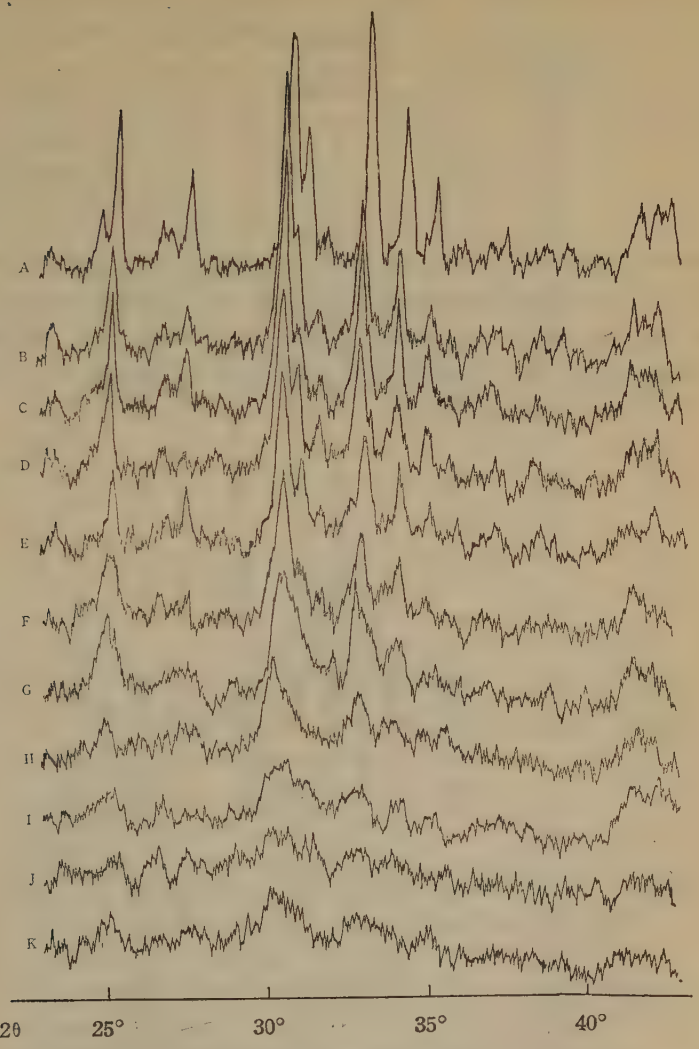

Fig. 1. Diffraction patterns of unheated allanite. Scan speed 1° per minute, scaler 4, time constant 8, chart speed ½ inch per minute.

A: Anak-ub. B: Ôyama-mura. C: Hakson-myon.
D: Kido-mura. E: Daimonji-yama. F: Mie-mura.
G: Hagata-mura. H: Tungwenchungtan. I: Kojima-mura.
J: Santaikou. K: Tafangshen.

Table 1. Spacings of unheated allanite. (Å)

hkl	Anak-ub	Dai-monji-yama	Mie-mura	Ôyama-mura	Haksan-myon	Kido-mura	Hagata-mura	Tung-wen-chung-tan	Kojima-mura	Santai-kou	Tafang-shen	Nogi-zawa-mura
201	3.239	3.252	3.251	3.255	3.258	3 258	3.267	3.273	—	—	—	—
$\left.\begin{matrix}\bar{1}13\\ \bar{3}02\end{matrix}\right\}$	2.916	2.940	2.933	2.933	2.943	2.943	—	2.965	—	—	—	—
020	2.872	2.887	2.892	2.902	2.902	2.900	2.907	2.914	—	—	—	—
211	2.816	2.828	2.831	2.838	2.837	2.837	2.837	2.844	—	—	—	—
$\left.\begin{matrix}013\\ 300\end{matrix}\right\}$	2.709	2.717	2.722	2.728	2.733	2.733	2.734	—	—	—	—	—
$\bar{3}11$	2.619	2.635	2.635	2.636	2.639	2.642	2.639	2.644	—	—	—	—
202	2.554	2.566	2.572	2.566	2.573	2.573	2 576	2.580	—	—	—	—
	1	5	6	2	3	4	7	8	9			

b) Heat-treated specimens: In order to observe the effects of heat treatment, the following samples were used:

Locality	Relative degree of the metamictization
Anak-ub	low
Mie-mura	middle
Kojima-mura	high

Heat-treated specimens were quenched and then subjected to X-ray spectrometry. The diffraction patterns obtained with unheated specimens and with those heat-treated both in the vacuum and in the air are shown in Figs. 2, 3 and 4*, and the spacings of the

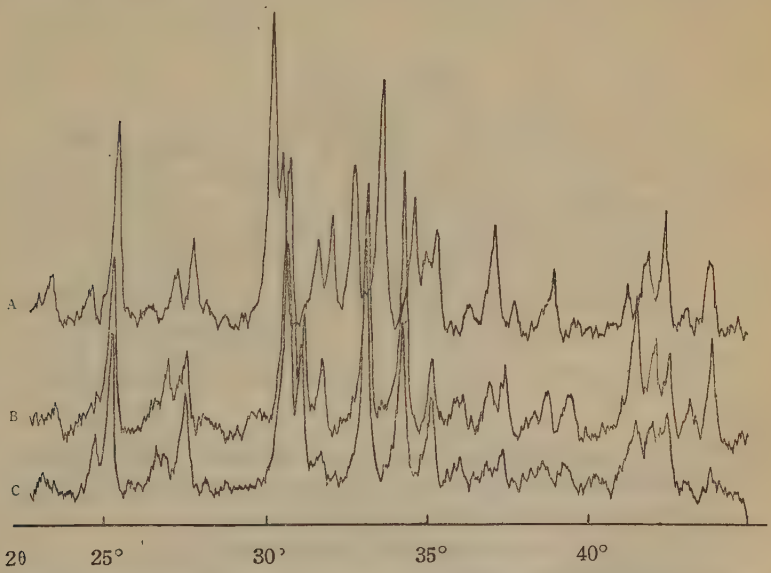

Fig. 2. Diffraction patterns of allanite from Anak-ub. Scan speed 1° per minute, scaler 4, time constant 8, chart speed ½ inch per minute.
A: heated in the air at 800°C for 2 hours.
B: heated in the vacuum at 800°C for 2 hours.
C: unheated.

* The effects of the heat treatment at about 400°C in the vacuum of the specimen from Anak-ub were not detectable. Hence, the diffraction pattern and the spacings have been omitted.

Table 2. Spacings of allanite from Anak-ub.

hkl	d_{unheated}	$d_{800°C}$	Δd	r
201	3.239Å	3.240Å	−0.001Å	−0.03
$\bar{1}13$ / $\bar{3}02$	2.916	2.909	0.007	0.2
020	2.872	2.870	0.002	0.1
211	2.816	2.819	−0.003	−0.1
013 / 300	2.709	2.704	0.005	0.2
$\bar{3}11$	2.619	2.617	0.002	0.1
202	2.554	2.554	0.000	0.0

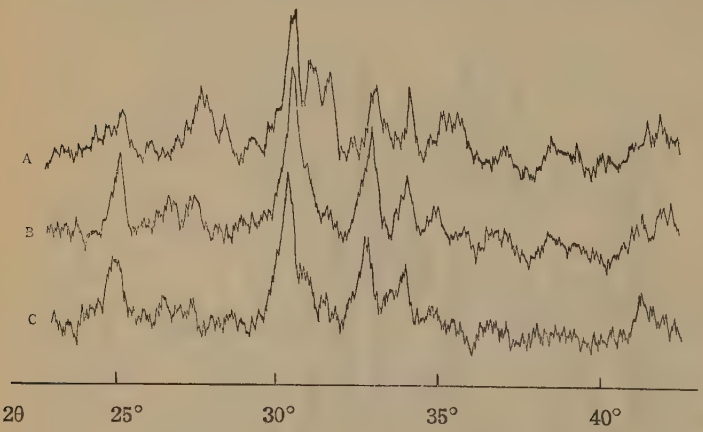

Fig. 3. Diffraction patterns of allanite from Mie-mura. Scan speed 1° per minute, scaler 4, time constant 8, chart speed ½ inch per minute.
A: heated in the vacuum at 800°C for 2 hours.
B: heated in the vacuum at 400°C for 2 hours.
C: unheated.

specimens heat-treated in the vacuum are given in Tables 2, 3 and 4*. In these tables, d_{unheated}, $d_{400°C}$ and $d_{800°C}$ denote the spacings of the specimens unheated, heat-treated at about 400°C and 800°C, both for two hours under the pressure of 10^{-4} mm Hg, respectively, and the other notations are as follows:

Table 3. Spacings of allanite from Mie-mura.

hkl	d_{unheated}	Δd_1	$d_{400°C}$	Δd_2	$d_{800°C}$	Δd	*r*
201	3.251Å	0.019Å	3.232Å	0.015Å	3.217Å	0.034Å	1.0
$\left.\begin{matrix}113\\ \bar{3}02\end{matrix}\right\}$	2.933	0.015	2.918	0.003	2.915	0.018	0.61
020	2.892	0.020	2.872	0.002	2.870	0.022	0.76
211	2.831	0.008	2.823	0.007	2.816	0.015	0.53
$\left.\begin{matrix}013\\ 300\end{matrix}\right\}$	2.722	0.013	2.709	0.008	2.701	0.021	0.77
$\bar{3}11$	2.635	0.016	2.619	0.000	2.619	0.016	0.61
202	2.572	0.014	2.558	0.010	2.548	0.024	0.93

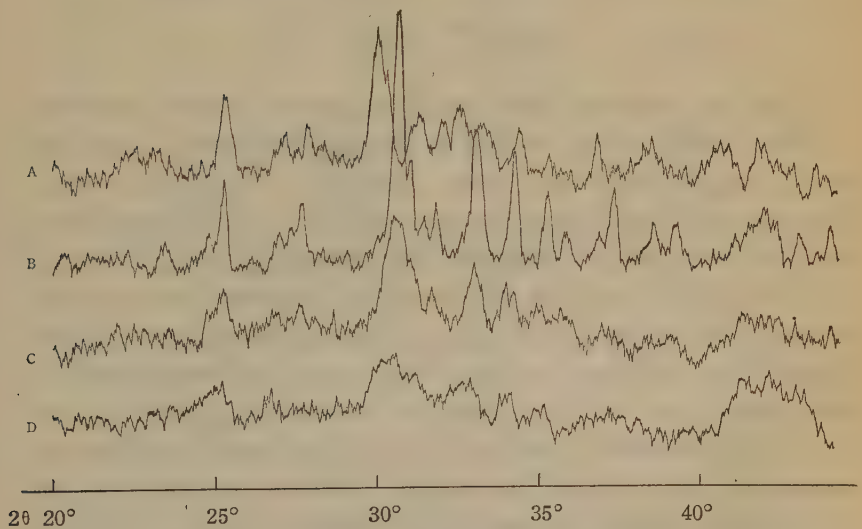

Fig. 4. Diffraction patterns of allanite from Kojima-mura. Scan speed 1° per minute, scaler 4, time constant 8, chart speed ½ inch per minute.

A: heated in the air at 800°C for 2 hours.
B: heated in the vacuum at 800°C for 2 hours.
C: heated in the vacuum at 400°C for 2 hours.
D: unheated.

Table 4. Spacings of allanite from Kojima-mura.

hkl	d_{unheated}	$d_{400°C}$	Δd_2	$d_{800°C}$
201	——	3.224Å	−0.001Å	3.225Å
$\left.\begin{matrix}\bar{1}13\\ \bar{3}02\end{matrix}\right\}$	——	2.916	0.007	2.909
020	——	2.878	0.000	2.878
211	——	2.816	0.008	2.808
$\left.\begin{matrix}013\\ 300\end{matrix}\right\}$	——	2.709	0.005	2.704
$\bar{3}11$	——	2.614	0.000	2.614
202	——	2.551	0.011	2.540

$\Delta d_1 = d_{\text{unheated}} - d_{400°C}$, $\Delta d_2 = d_{400°C} - d_{800°C}$, $\Delta d = d_{\text{unheated}} - d_{800°C}$,

and $$r = \frac{\Delta d}{d_{\text{unheated}}} \times 100 .$$

As will be seen from these results, the effects of heat treatment at about 800°C in the vacuum on the specimen from Anak-ub revealed a slight lattice contraction, whereas on the specimens from Mie-mura and Kojima-mura not only considerable lattice contractions but also increases of sharpness and decreases of the degree of asymmetry of the peaks in the diffraction patterns. These results indicate that the heat treatment of the specimens in the vacuum causes their structures to recover their normal lattice states*, and the greater part of the recovery in the specimens from Mie-mura can be accomplished below 400°C, which will easily be seen by comparing the values of Δd_1 and Δd_2. However, the effects of the heat treatment in the air show quite different results. The most remarkable is the appearance of new peaks. This means that the effect of the heat treatment of the specimen in the air is irreversible.

* Here and in the following sections, the authors refer with the words, "normal lattice state" to the structures of certain specimens of respective minerals which give sharp X-ray diffraction patterns peculiar to ordered structures.

Gadolinite

In Fig. 5 are shown the diffraction patterns of gadolinite from Arendal, unheated and heat-treated both in the vacuum and in the air, and the spacings are listed in Table 5. The indices in the first

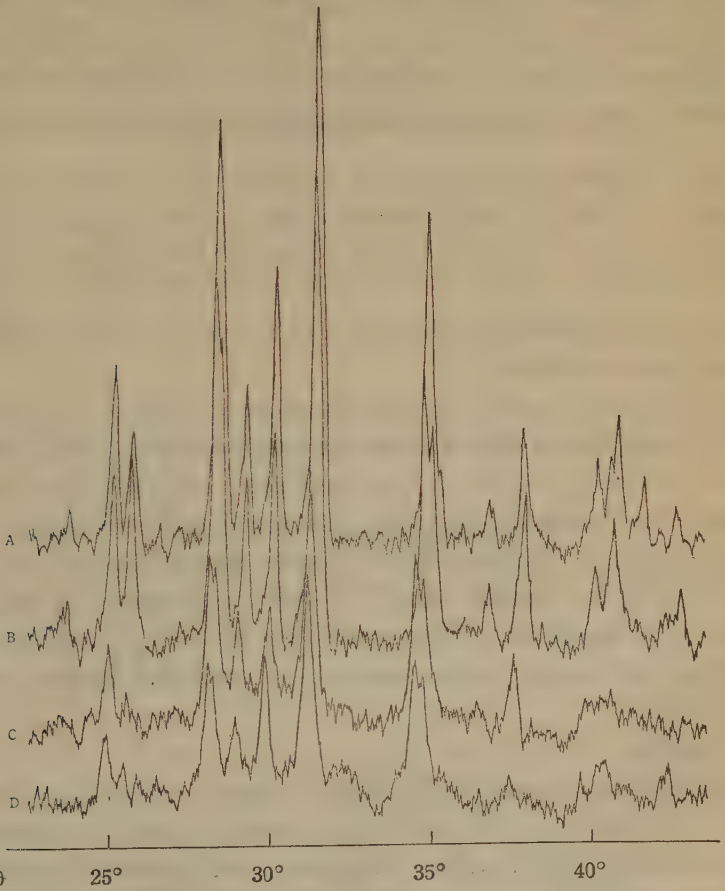

Fig. 5. Diffraction patterns of gadolinite from Arendal. Scan speed 1° per minute, scaler 4, time constant 8, chart speed ½ inch per minute.

A: heated in the air at 800°C for 2 hours.
B: heated in the vacuum at 800°C for 2 hours.
C: heated in the vacuum at 400°C for 2 hours.
D: unheated.

Table 5. Spacings of gadolinite from Arendal.

hkl	d_{unheated}	Δd_1	$d_{400°C}$	Δd_2	$d_{800°C}$	Δd	r
$\bar{1}12$	3.171Å	0.003Å	3.168Å	0.029Å	3.139Å	0.032Å	1.0
112	3.153	0.003	3.150	0.025	3.125	0.028	0.89
013	3.082	0.010	3.072	0.031	3.041	0.041	1.3
120	2.984	0.009	2.975	0.023	2.952	0.032	1.1
$\bar{1}21$ 121	2.864	0.004	2.860	0.026	2.834	0.030	1.0
$\bar{1}13$ 113	2.597	0.002	2.595	0.027	2.568	0.029	1.1
$\bar{1}22$ 122	2.580	0.004	2.576	0.022	2.554	0.026	1.0
031	2.464	0.000	2.464	0.028	2.436	0.028	1.1
200	2.400	0.008	2.392	0.026	2.366	0.034	1.4

column in the table are calculated with the lattice constants determined by Ito and Mori[4].

In this case, the effects of heat treatments both in the vacuum and in the air revealed a considerable lattice contraction, an increase of the sharpness of the diffraction patterns and a decrease of the degree of asymmetry of the peaks. There is, however, no appearance of new peaks as in the case of allanite heat-treated in the air. Accordingly, the change caused by heat treatments of gadolinite seems to be reversible. The greater part of the recovery of this specimen to its normal lattice state was accomplished between 400°C and 800°C.

Monazite

In Fig. 6 are shown the diffraction patterns of monazites from Kobe-mura and from Harimichi-mura, unheated and heat-treated in the vacuum*. The spacings calculated from the peaks in the diffraction patterns are given in Tables 6 and 7*. The indices in the first columns in these tables are derived from the lattice constants

* The effects of the treatment at about 400°C in the vacuum on the specimen from Harimichi-mura were not detectable. Hence, the diffraction pattern and the spacings have been omitted.

determined by Ueda[11].

As will be seen from these results, the specimen from Kobe-mura has, in its raw state, larger spacings than that from Harimichi-mura, while there is no appreciable difference in sharpness between these two. The results of heat treatments in the vacuum show lattice contraction, at a greater degree with the specimen from Kobe-mura than that from Harimichi-mura. It seems, consequently, that the lattices of these specimens are also expanded under the

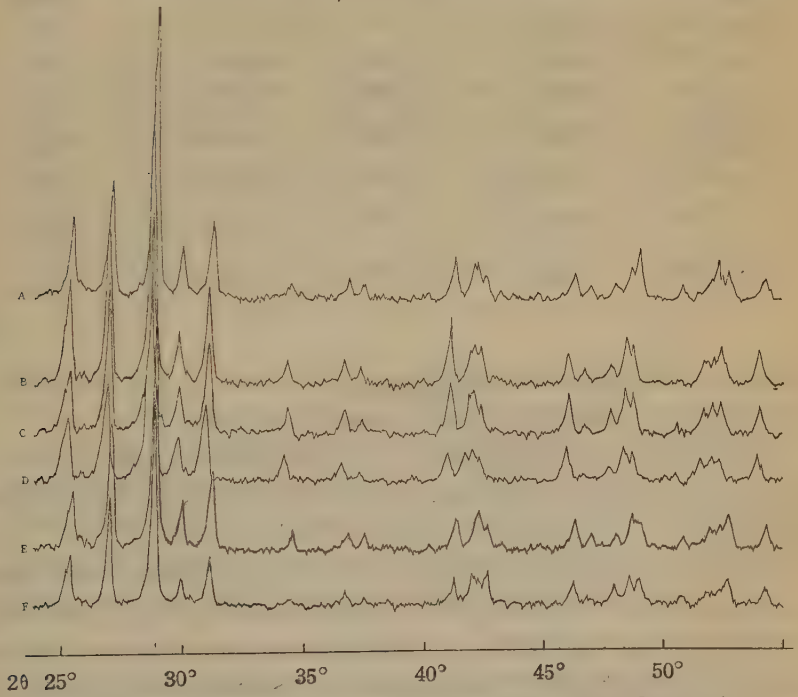

Fig. 6. Diffraction patterns of monazite. Scan speed 1° per minute, scaler 8, time constant 8, chart speed ½ inch per minute.
A: heated in the air at 800°C for 2 hours (Ishikawa-machi).
B: heated in the vacuum at 800°C for 2 hours.
C: heated in the vacuum at 400°C for 2 hours. } (Kôbe-mura).
D: unheated.
E: heated in the vacuum at 800°C for 2 hours.
F: unheated. } (Harimichi-mura).

Table 6. Spacings of monazite from Harimichi-mura.

hkl	d_{unheated}	$d_{800°C}$	Δd	r
200	3.294Å	3.286Å	0.008Å	0.2
120	3.086	3 086	0.000	0.0
012	2.867	2.860	0.007	0.2
$\left.\begin{matrix}\bar{1}12\\112\end{matrix}\right\}$	2.600	2.595	0.005	0.2
220	2.396	2.394	0.002	0.1
$\left.\begin{matrix}113\\031\end{matrix}\right\}$	2.184	2.179	0.005	0.2
212	2.148	——	——	——
310	2.116	2.117	−0.001	−0.05
311	1.960	1.956	0.004	0.2
$\left.\begin{matrix}230\\222\end{matrix}\right\}$	1.899	1.891	0.008	0.4
032	1.872	1.867	0.005	0.3
$\left.\begin{matrix}\bar{1}23\\312\end{matrix}\right\}$	1.735	1.733	0.002	0.1
$\left.\begin{matrix}140\\041\end{matrix}\right\}$	1.688	1.680	0.008	0.5

influence of metamictizing agents as in the case of the two radioactive minerals described in the foregoing sections.

The greater part of the recovery to the normal lattice structure in the specimen from Kobe-mura is completed below 400°C, which can be seen by comparing the values of Δd_1 and Δd_2.

The effects of heat treatment in the air on monazite were also examined with a specimen from Ishikawa-machi as well as with those now under consideration, and the results are given in Fig. 6. Apart from slight mutual displacements of corresponding peaks in these patterns, no appreciable difference is found between the patterns of the heat-treated specimens and those of the unheated ones. This suggests that the change in monazite caused by heat treatment in the air is reversible as in the case of gadolinite.

Table 7. Spacings of monazite from Kôbe-mura.

hkl	d_{unheated}	Δd_1	$d_{400°C}$	Δd_2	$d_{800°C}$	Δd	r
200	3.310Å	0.011Å	3.299Å	0.000Å	3.299Å	0.011Å	0.33
120	3.107	0.011	3.096	0.004	3.092	0.015	0.48
012	2.887	0.015	2.872	0.002	2.870	0.017	0.59
$\bar{1}12$ 112	2.619	0.009	2.610	0.006	2.604	0.015	0.57
220	2.410	0.008	2.402	0.000	2.402	0.008	0.3
113 031	2.198	0.009	2.189	0.000	2.189	0.009	0.4
212	2.148	0.007	2.141	0.001	2.140	0.008	0.4
310	2.131	0.004	2.127	0.000	2.127	0.004	0.2
311	1.971	0.005	1.966	−0.001	1.967	0.004	0.2
230 222	1.904	0.005	1.899	0.001	1.898	0.006	0.3
032	1.880	0.004	1.876	0.003	1.873	0.007	0.4
$\bar{1}23$ 312	1.747	0.004	1.743	0.002	1.741	0.006	0.3
140 041	1.698	0.003	1.695	0.002	1.693	0.005	0.3

Conclusion

From the experimental results described above, it is to be concluded that among three radioactive minerals under consideration, allanite and gadolinite become into metamict states through the process of lattice expansion; while monazite goes as far as lattice expansion under the influences of metamictizing agents.

The authors wish to express their sincere thanks to Professor T. Ito of the University of Tokyo for providing facilities for their use of the Norelco X-ray Spectrometer.

REFERENCES

1) Arnott, R. J.: Am. Miner., **35**, 386 (1950).
2) Hurley, P. M. and H. W. Fairbairn: Bull. Geol. Soc. Am., **64**, 659 (1953).
3) Hutton, C. O.: Bull. Geol. Soc. Am., **61**, 635 (1950).

4) Ito, T. and H. Mori: Acta Cryst., **6**, 24 (1953).
5) Machatschki, F.: Centralblatt Min., Abt. A, 38 (1941).
6) Pabst, A.: Am. Miner., **36**, 60 (1951).
7) Pellas, P.: Compt. rend., **233**, 1369 (1951).
8) Pellas, P.: Compt. rend., **234**, 538 (1952).
9) Stech, B.: Z. Naturforsch., **7a**, 175 (1952).
10) Tomkeieff, S. I.: Science Progress, **36**, 136, 696 (1946).
11) Ueda, T.: Memoirs Coll. Sci. Univ. Kyoto, B, **20**, 227 (1953).
12) Ueda, T. and M. Korekawa: Memoirs Coll. Sci. Univ. Kyoto, B, **21**, 151 (1954).
13) Ueda, T.: unpublished.

Manuscript received January 8, 1955.

MINERALOGICAL JOURNAL, VOL. 1, NO. 4, PP. 213-223, JUNE, 1955

THE DEVELOPMENT OF PLEOCHROIC HALOES AND THE ALPHA RADIOACTIVITY OF THE NUCLEUS MINERALS*

ICHIKAZU HAYASE

Geological and Mineralogical Institute, Faculty of Science, University of Kyoto

ABSTRACT

The pleochroic halo has been regarded as the index of the geologic age of rocks, especially of granite. The autoradiographic studies now enable us to measure the alpha radioactivity even of a single grain of minute mineral and to determine more perfectly the evolution of the halo produced around it. Thus the geologic age of a rock can be determined more easily. In this paper are treated the development of haloes and the radioactive homogeneity of the minute minerals in their nuclei.

Introduction

The varieties of minute radioactive minerals contained in thin sections of granite were examined by an autoradiographic method, with the nuclear emulsion ET-2E (Fuji Photo Film Co. Ltd.). From this test the author was informed that the varieties of minute radioactive minerals were included in granite and that two grain belonging to the same variety were often quite different in their radioactive order[2].

To be measured by this method are the alpha tracks expelled from each grain of such minute minerals. If such a grain has been included in biotite, there is always to be seen a pleochroic halo, whose blackness depends upon the alpha radioactivity of the grain as well as upon the geologic age of the grain and accordingly of

* Read at the meeting of the Kansai Branch of the Geological Society of Japan, on September 25, 1954.

the rock in which it is contained. In other words, such a halo is the autoradiographic image which the radioactivity of the mineral in the nucleus has left, for a long geologic age, upon its surrounding biotite. So the radioactivity of the mineral and the pleochroic halo produced around them were studied by the author to determine the geologic age of the rocks[3], and also as a contribution to studies on petrogenesis.

Heterogeneity in minute radioactive minerals

Concerning the distribution of radioactive elements in a mineral, von Buttlar[1] already pointed out its heterogeneity. The present author, by means of NaF beads, also found this kind of heterogeneity in minute zircon grains[4].

Microscopic observation of granite often furnishes us some abnormally formed pleochroic haloes, some of which are more developed at one end than at the other of an acicular zircon crystal, and others growing only by halves around the crystal, where we might expect a full one all around it. These facts tell us of the heterogeneous distribution of radioactive elements even in a minute mineral. This heterogeneity will be treated, later on, together with the relation between pleochroic haloes and the radioactivity of the minerals in the nuclei. In case of larger minerals[1] this heterogeneity is often evident from the heterogeneous distribution of the alpha tracks emitting out of that mineral.

Owing to this heterogeneity, the relation of the radioactivity of a mineral to the pleochroic halo printed around it must be studied statistically through a carefull observation of many samples.

Pleochroic halo and the size of the nucleus mineral

If the nucleus mineral is very small in size and the circumstances ar efavourable, the pleochroic halo will consist of dual or more

rings, owing to the varieties of the range of alpha particles. Even in the same granite, pleochroic haloes can often be multifarious, since the nucleus minerals are different from each other both in size and in shape. It is to be noticed that the halo depends only upon the residual range of each alpha particle reaching outside the surface of the mineral, and not upon the total number of the particles emitted from the mineral. Hence, the smaller the size of nucleus mineral is, the more efficiently the halo is developed, owing to the small absorption of alpha particles. In regard to haloes, however, the alpha permeabilities of various nucleus minerals deserve no serious consideration, for there is only a slight variation among them.

In this investigation the nucleus minerals were divided into two heads:

a) those whose size exceeds 40 microns, and

b) those whose size is less than 40 microns.

a) In case the size of the mineral exceeds the longest range of the alpha particles, some of them which have started from the center of the mineral, being absorbed inside the mineral itself, fail

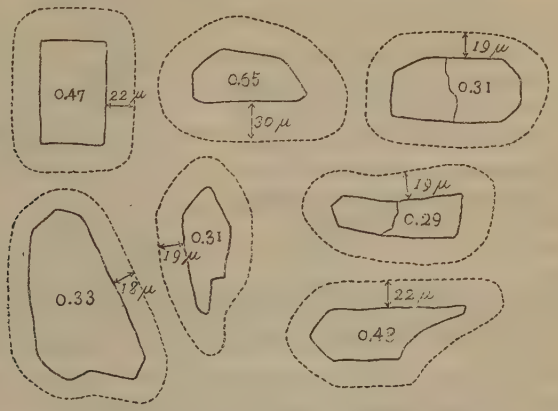

Fig. 1. Zonal pleochroic haloes and the alpha radioactivities of their nucleus minerals. (Mikumo Granite)
The dotted lines show the pleochroic halo boundary and the number in the center, the alpha track population (T_∞).

to affect the surrounding biotite. In this case the size of the mineral must be larger at least than 40 microns, slightly variable as it may be, in accordance with the alpha permeability of the mineral and as to whether uranium or thorium its radioactive content is. Here, the radioactive elements are, of course, supposed to be homogeneously distributed throughout the mineral.

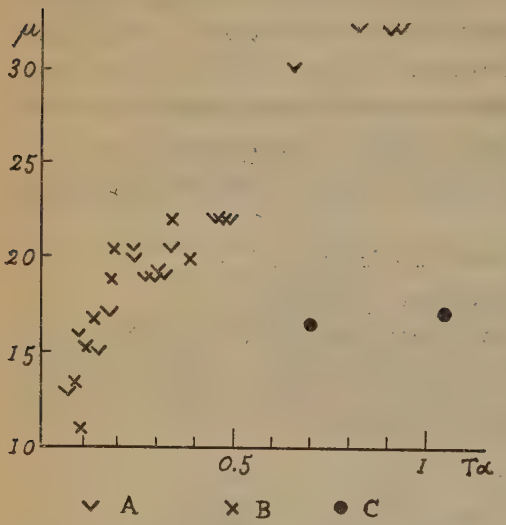

Fig. 2. The relation between the widths (μ) of zonal pleochroic haloes and the alpha radioactivities (T_α) of their nucleus minerals.
A: Mikumo Granite. B: Konze Granite. C: Tango Granite.

For example, the author examined the pleochroic haloes in the granite samples from Mikumo and Konze, Shiga Prefecture, and obtained the following results. As illustrated in Figs. 1 and 2, between the alpha track population (T_α)* of the mineral in the nucleus and the width of the halo surrounding it, there is a very regular relation, namely: if T_α is 0.2~0.5, then the halo width is 20~22 microns, and if T_α is 0.1~0.2, the halo width is 14~19 microns. The halo has probably been produced, in the former case, by RaA and other elements with the similar range of alpha particles, while, in the latter by RaF and its group. Only when T_α exceeds 0.6, we find the largest halo that RaC′, one of the uranium series, has produced.

The points representing the relation between the width of zonal

* $T_\alpha = \psi\ (25.73\ U + 7.80\ Th)$[5] where ψ: alpha permeability, U: uranium content (g/g), and Th: thorium content (g/g).

pleochroic haloes and the alpha radioactivity of the nucleus minerals in the Mikumo and Konze Granite samples fall in the same zone, as illustrated in Fig. 2. Therefore, it may be inferred that the two granite samples are of similar geologic age[3]. Dotted marks falling in the right region in Fig. 2 suggest a younger geologic age of the Tango Granite than the Mikumo one[3]. The determination of geologic age by using these relations is possible in case that radioactive elements are distributed throughout the nucleus mineral homogeneously or, at least, more homogeneously than in those heterogeneous cases to be alluded to afterward.

b) Nucleus minerals whose size is less than 40 microns. Even in case of a nucleus mineral exceeding 40 microns, halo has grown sometimes only on an edge, sometimes only along a plane, of that crystal. In nucleus minerals whose size are less than 40 microns, this tendency is more remarkable: different grain shapes have produced much differently shaped haloes.

Examples of haloes found in the same Konze Granite sample are given in Fig. 3, in which a comparatively regular relation is to be seen between the alpha radioactivity of nucleus minerals and the radii of haloes. For brevity's sake, the grain shapes being exempted for a while, the grain sizes alone were compared with each other in Fig. 3. As evident from estimation curves in Fig. 3, grains with similar cross-sections show rather regular tendency resembling the relation presented in Fig. 2, while the curve corresponding smaller grain are shifted toward the lower right region of the figure. Even grains with similar cross-sections might have produced, according to their different shapes, differently developed zonal haloes and offer us as shown in Fig. 3 a distribution more irregular than that presented in Fig. 2.

The positions of nucleus minerals, especially with diameters less than 30 microns, in the thin section deserve special consideration; that is, the thickness of the thin section being about 30 microns, diverse positions of minerals in it can bring about a great variability

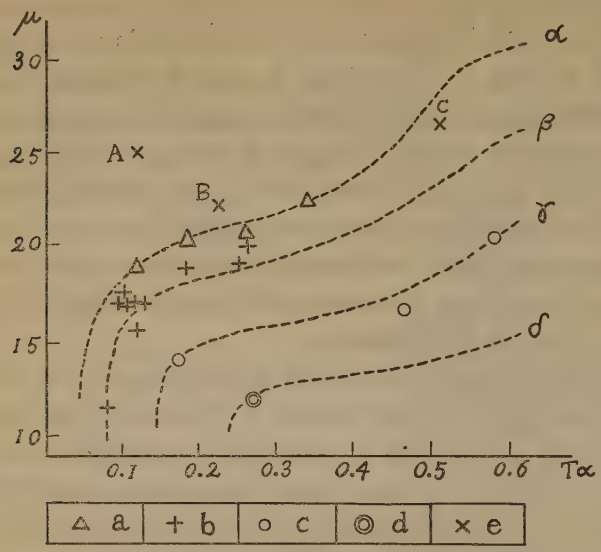

Fig. 3. The relation between the radii (μ) of haloes and the alpha radioactivities (T_α) of the nucleus minerals whose sizes are less than 40 microns. (Konze Granite)

a: nucleus minerals with cross-sections $(0.225 \pm 0.012) \times 10^{-2}$ mm².
b: ditto $(0.104 \pm 0.002) \times 10^{-2}$ mm².
c: ditto $(0.043 \pm 0.002) \times 10^{-2}$ mm².
d: ditto 0.02×10^{-2} mm².
e: extraordinary halo.
α: estimation curve for nucleus minerals with cross-sections about 0.2×10^{-2} mm².
β: ditto 0.10×10^{-2} mm².
γ: ditto 0.04×10^{-2} mm².
δ: ditto 0.02×10^{-2} mm².

of the track population printed upon the nuclear emulsion, as shown in Fig. 4. Whether a mineral is situated at the top of, or included in, or hidden under, a biotite layer, can easily be determined by the interference colour observed under the open nicol.

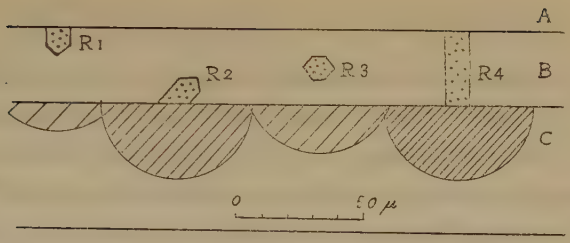

Fig. 4. Transversal section of the autoradiography of minute minerals.
A: slide glass.
B: thin section of rock.
C: nuclear emulsion.
R1: minute mineral burried deep in the thin section.
R2: ditto, lying only on the surface of the thin section.
R3: ditto, included entirely in the thin section.
R4: ditto, occupying the full thickness of the thin section.
The shadow-lined area are the scopes of alpha particle injection, and the line density indicates the relative number of alpha track in the emulsion.

Extraordinary pleochroic haloes

It is to be noted that there are found some haloes larger or darker than those proper to the size and the radioactive order of their nucleus minerals; this disproportion informs us of the specific condensation of radioactive elements particularly in a part, such as on the surface, of the nucleus mineral, though the irregularity may be more or less relevant to the orientation of nucleus mineral and halo in the section.

A, B and C in Fig. 3 are the examples of the extraordinary haloes. These haloes do not fall in the zone proper to them in respect to the size of the nucleus minerals and the halo radii, but shift to upper left region of the figure; in other words, the development of those haloes is far more intense than due to the radioactive order of their nuclei. This tendency rather suggests the concentration of radioactive elements on the surface of the nucleus minerals.

Pleochroic haloes in the Kitashirakawa Granite

This adamellitic granite lies as a stock in the region extending from the east part of Kyoto City to Ootsu City, and intrudes into a Palaeozoic Formation probably of the Permo-Carboniferous Period.

The pleochroic haloes of zonal type, found in the thin sections of this granite were studied with special attension to the following points:

1) The width of halo must be measured, not at its curved part, but at its straight part whose length exceeds, at least, about 40 microns.

2) For the strict measurement of the width, only such halo of which the nucleus mineral shows rectangular cross-section, must be chosen. In case the nucleus mineral is cut otherwise, the halo width must be measured at its narrowest part, to obtain the true width of that halo. The position of the nucleus and its halo in a thin section must also be taken into consideration.

3) It is most desirable, whenever possible, to compare with each other the haloes growing around the nucleus mineral of the same kind.

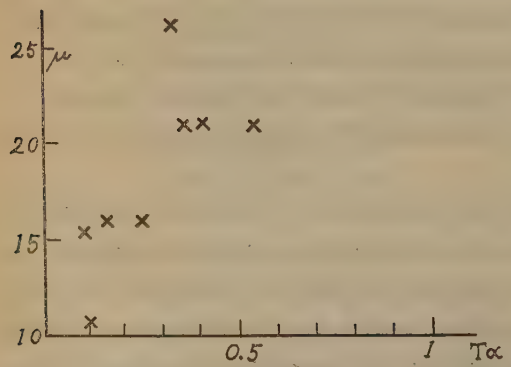

Fig. 5. The width of zonal type plcochroic halo and the alpha radioactivity of the nucleus mineral. (Kitashirakawa Granite)

4) Biotite crystals with similar colour and optical character are most suitable for comparing the haloes included in them.

Taking into consideration these points, the zonal haloes of the Kitashirakawa Granite were compared with each other and the results are illustrated

in Fig. 5, in which RaC′ zonal haloes about 32 microns in width are scarcely seen; for comparatively coarse grained nucleus minerals which produce zonal haloes around them are all so feebly radioactive. Mostly the pleochroic haloes 22~23 microns in width are connected with the radioactivity whose alpha track population (T_α) is about 0.36~0.53, and haloes 15~16 microns in width, with that of T_α=0.09 ~0.25. A halo 27 microns in width and of ThA origin was observed around a grain whose radioactivity (T_α) was 0.32. Grains with radioactivity (T_α) not exceeding 0.09 have produced around them only very faint haloes with width less than 10 microns. Fig. 5 implies the data of some biotite samples that have changed into chlorite, but not much deviated, so far as known to the author, from the fresh biotite in their halo development.

Now, let us turn to nucleus minerals smaller than 40 microns in size. In this case also, the haloes containing radioactive grains with similar alpha-permeability and of similar shape and size are the best for comparing with each other, because the absorption of alpha particle energy by the grains themselves affects the development of haloes.

In fact, the most preferable are the disk haloes developed around zircon crystals with their basal sections of about 30 microns square; for they are the most abundant of all the generators of disk haloes in Kitashirakawa Granite and they show much diversity in their radioactivity. The data obtained for them revealed a relatively regular relation between the radioactivity and the halo development, as illustrated in Fig. 6. (The repetition of 4 weeks' autoradiographic exposure assured us of a high coincidence concerning the total alpha track number emitting from the same grain.)

The autoradiographic study of granite masses, whose geologic age is already known, will soon clarify how many alpha particles had played their role, before a halo attained to a certain degree of its development. So far as the Kitashirakawa Granite is concerned, a RaC′ halo about 32 microns wide is seen around a grain emitting

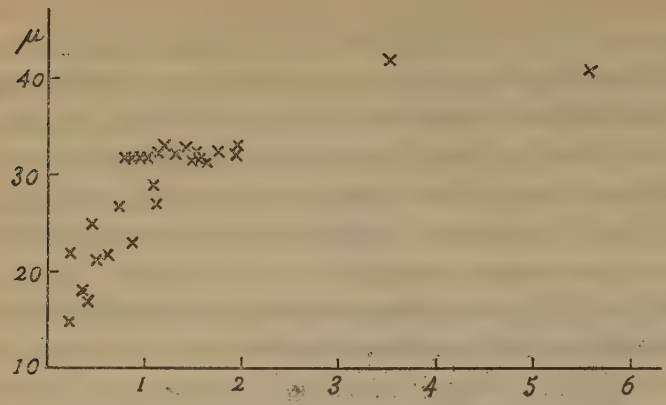

Fig. 6. The radii of disk type pleochroic haloes and the alpha radioactivities of the nucleus minerals about 30 microns square in the cross-section. (Kitashirakawa Granite)
The radioactivity is indicated by the number of the alpha particles emitted per one grain per day.

2.0~0.8 alpha particles daily, and another halo 22~18 microns wide around a grain emitting 0.9~0.2. Two ThC′ haloes some 41 microns wide were found, in rare cases, around grains each emitting 3.5 and 5.6 alpha particles daily. Some obliquely orientated nucleus minerals can be found in the thin sections and serve as further materials for our comparison, provided that enlarged sections are first calibrated.

Summary and Conclusion

1. The relation between the nucleus radioactivity and the halo development was determined by observations upon the nucleus minerals of which the distribution of radioactive elements are homogeneous.

2. The development of zonal haloes around nucleus minerals larger than 40 microns in size is dependent, with comparatively high regularity, solely upon the radioactive order of the nucleus minerals, and quite independent upon their grain size and shape.

3. As for the nuclei smaller than 40 microns in size, there is also a certain regularity between the nucleus radioactvity and the halo development, although there are some exceptions even if their grain sizes are alike.

4. An extraordinarilly developed pleochroic halo in comparison with the radioactive order of the mineral reveals the heterogeneous distribution of radioactive elements, namely, their excessive concentration on its surface, or even in a part of its surface.

Acknowledgements

The author expresses his hearty thanks to Professor A. Harumoto, Professor S. Matsushita and Assist. Professor Jin. Hatuda, of the Geological and Mineralogical Institute, University of Kyoto, and to Professor K. Kimura, Physical Institute of the University of Kyoto, for their valuable help and advice in carrying out this work. He is also indebted to Dr. S. Fujizawa and Mr. S. Koseki of the Research Laboratory, Fuji Photo Film Co. Ltd., for supplying him with ET-2E plates. Funds necessary for this investigation has been partly defrayed by the Scientific Grant of the Ministry of Education and by the Grant of the Hattori Hôkôkai, to which the author wishes to express his thanks.

REFERENCES

1) von Buttlar, H. and F. G. Houtermans: Geochi. Cosmochi. Acta, **2**, 43, (1951).
2) Hayase, I.: Mem. Coll. Sci. Univ. Kyoto, Ser. B, **20**, 247, (1953).
3) Hayase, I.: Amer. Mineral., **39**, 761, (1954).
4) Hayase, I.: Mineral. Jour., **1**, 147, (1954).
5) Yagoda, H.: Radioactive Measurements With Nuclear Emulsions, (New York, John Wiley, 1949).

Manuscript received January 8, 1955.

MINERALOGICAL JOURNAL, VOL. 1, NO. 4, pp. 224–232 JUNE, 1955

IRON-RICH CHLORITE FROM SHŌGASÉ, KŌCHI PREFECTURE, JAPAN

HARUO SHIROZU

Department of Geology, Faculty of Science, Kyushu University

ABSTRACT

Chemical, X-ray, and thermal analyses along with petrographical data are given for a specimen of iron-rich chlorite from Shōgasé, Kōchi Prefecture, Japan. The X-ray data are given also for "chamosite" from the Arakawa mine, Japan. X-ray powder lines, which are indexed on the basis of an ortho-hexagonal cell, together with the thermal data, confirmed that the structure cell of this mineral was similar to that of "chamosite" from Schmiedefeld, Thuringia as suggested by Engelhardt. Some notes on the nomenclature are presented.

Occurrence and general properties

The chlorite was collected during the geologic research for fire-brick silica stone deposits* at Shōgasé, Sanze Village, Agawa County, Kōchi Prefecture**, Japan, in 1952. The deposits are found along a contact between diabasic intrusives and the Palaeozoic sediments as quartzite and schalstein. The chlorite occurs as dark green films either along the outer boundary of the deposits or filling fissures in the wall rocks. Along the chlorite films, the wall rock is dark

* The silica stone is known by the commodity name of "Akashiro keiseki" (red and white silica stone) in Japan. They appear dapple, consisting of the angular fragments of hematite-bearing fine-grained reddish-colored cherty rocks, and the white-colored coarse-grained vein quartz. Some of them look similar to a loin of beef. Substitution of green-colored cherty fragments for the reddish ones is common, and in this case chlorite appears in places of hematite. These iron-containing silica stones have been successfully used in Japan as the raw materials for silica bricks.

** 高知県吾川郡三瀬村勝賀瀬

terruginous color and consists of microcrystalline quartz, chlorite and mica (iron-sericite ?).

The chlorite is dark green in color, fine scaly in habit, arranged subparallel to the wall rock, vitreous in luster. Pleochroism distinct: X pale greenish yellow, Y and Z green. The refractive indices: α=1.634, γ=1.652, $\gamma-\alpha$=0.018. Apparent optic angle of crystal aggregates is zero to very small; optically negative.

The specific gravity was determined as 3.10 with about 2 grams of sample by means of a picnometer.

Chemical Composition

The results of the chemical analysis are given in Table 1, Column 1, together with some other earlier analyses on chlorite. As written in the later pages "chamosites" in Columns 2 and 3,

Table 1. Chemical analyses of some iron-rich chlorites.

	1	2	3	4	5	6
SiO_2	24.56%	24.50%	26.65%	24.18%	20.82%	24.78%
TiO_2	none		tr.		tr.	
Al_2O_3	16.07	16.32	16.14	18.23	17.64	18.69
Fe_2O_3	5.10	7.45	6.69	10.56	8.70	6.45
FeO	34.66	31.46	34.43	29.75	37.96	36.17
MnO	1.42	3.33		0.48		
MgO	6.16	4.59	4.47	5.40	4.15	4.52
CaO	0.30			0.24		
$H_2O(+)$	11.93	11.36	11.42	9.54	10.31	9.09
$H_2O(-)$	0.54		0.08	1.07	0.07	
Total	100.74%	99.01%	99.88%	99.45%	99.65%	99.70%

1. Chlorite from Shōgasé, Kōchi Prefecture, Japan. Analyst: H. Shirozu.
2. "Chamosite" from the Arakawa mine, Akita Prefecture, Japan[11].
3. "Chamosite" from Schmiedefeld, Thuringia[9].
4. Thuringite from Evisa (Corse)[10].
5. Thuringite from Schmiedefeld, Thuringia[8].
6. Aphrosiderite from Striegau.[12]

have the similar structure cells to this chlorite. Thuringites in Columns 4 and 5, and aphrosiderite in Column 6 are chemically similar to this mineral.

Structural formula and theoretical density

From the chemical analysis in Table 1, column 1, the structural formula is calculated. Assigning O and (OH) ions to the 18 positions in the ideal structure, the formula is:

$$\underbrace{(Ca_{0.03}Mg_{1.01}Mn_{0.13}Fe^{2+}_{3.21}Fe^{3+}_{0.42}Al_{0.82})}_{5.62\ \text{atoms}}\ \underbrace{(Si_{2.72}Al_{1.28})}_{4\ \text{atoms}}\ \underbrace{O_{9.20}(OH)_{8.80}}_{18\ \text{atoms}}$$

The discrepancies between the ideal chlorite formula, $(R_{6-n}Al_n)(Si_{4-n}Al_n)O_{10}(OH)_8$, are: (i) excess of (OH), (ii) deficiency of octahedral cations, (iii) disparity between tetrahedral and octahedral Al ions. These points need further research.

From the structural formula and the cell dimensions described later, the theoretical density can be calculated. The molecular weight is 665.8. Its volume is 710.1/2 Å^3. The theoretical density is then 3.11, in excellent agreement with the observed value (Sp. Gr.=3.10).

X-ray powder diagrams

X-ray powder diagrams for Fe $K\alpha$(λ=1.9373Å) radiations were obtained with a 114.6 mm. diameter camera. In addition to the

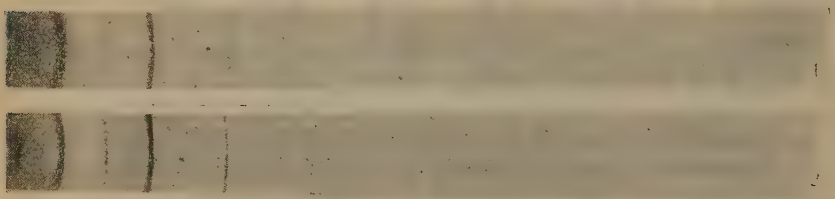

Figs. 1-2. Powder photographs of ortho-hexagonal iron-rich chlorites.
1. Chlorite from Shōgagé.
2. "Chamosite" from the Arakawa mine.

chlorite from Shōgasé, a specimen of "chamosite" from a quartz vein of the Arakawa mine, recently described by T. Sudo[11] was also examined.

The diagrams are shown in Figs. 1 and 2. The measured lattice

Table 2. X-ray powder data for ortho-hexagonal iron-rich chlorites.

	1			2			3		4	
hkl	*I*	$d_{obs.}$(Å)	$d_{calc.}$(Å)	*I*	$d_{obs.}$(Å)	$d_{calc.}$(Å)	*I*	*d*(kX)	*I*	*d*(kX)
001	2	14.1	14.16	4	14.1	14.17			3	14
002	10	7.05	7.08	10	7.05	7.09	10	6.62	10	6.93
003	2B	4.46	4.72	4	4.71	4.72	5	4.54	5	4.63
020			4.66			4.68				
022				½	3.92	3.90				
004	8	3.53	3.54	8	3.53	3.54	8	3.47	9	3.50
005	½	2.83	2.832	3	2.84	2.834	2	2.78	3	2.779*
024			2.818			2.823				
200	3	2.67	2.691	1	2.70	2.699			1	2.689
201	½	2.63	2.640	½	2.67	2.651				
202	5§	2.50	2.515	5	2.52	2.522	5	2.50	7	2.507
025	¼	2.42	2.420						½	2.330
204	2§	2.14	2.142	4	2.15	2.147	5	2.14	3	2.134
007	¼	2.02	2.023	1	2.023	2.024				
206	1	1.76	1.775	3	1.778	1.777	5	1.77	2	1.767
240			1.761			1.768				
207				¼	1.63	1.619				
060	5	1.553	1.553	4	1.558	1.558	2	1.56	5	1.556
062	3	1.517	1.517	2	1.522	1.522	5	1.52	2	1.524
208	½	1.477	1.479	3	1.479	1.481	2	1.48	1	1.473
063			1.475			1.480				
064	1B	1.419	1.422	1	1.424	1.426	2	1.42	1	1.425
0010			1.416	2	1.417	1.417				
209				¼	1.359	1.360				
401	½	1.340	1.339	½	1.344	1.343				
402	1	1.319	1.321	1	1.325	1.326				
066	½	1.299	1.298	½	1.300	1.301				

Table 2.—*Continued*

404			1.257	½	1.259	1.261		
	¼	1.255					2	1.26
2010			1.253	1	1.255	1.255		
0012	½	1.180	1.180	1	1.181	1.181	2	1.18
				½	1.171			
				½	1.081			
				½	1.074			
	½	1.045		1	1.047		1	1.05
	½	1.010		2	1.011		1	1.01

Equivalent indices: $02l = 11l$; $20l = 13l$; $24l = 15l = 31l$; $06l = 33l$; $40l = 26l$.

1. Chlorite from Shōgasé. Fe $K\alpha$, $\lambda = 1.9373$Å. Camera radius 57.3 mm. B: an unusually broad line. § The head of a diffused band extending to the side of smaller spacings.
2. "Chamosite" from the Arakawa mine. Fe $K\alpha$, $\lambda = 1.9373$Å. Camera radius 57.3 mm..
3. "Chamosite" from the Arakawa mine. Data by Sudo[11]. Co K. Camera radius 28.65 mm.. The readings were not calibrated. The 14 Å line was not recorded owing to the small radius of the camera.
4. "Chamosite" from Schmiedefeld, Thuringia. Data by Engelhardt[5] Fe $K\alpha$. Camera radius 57.5 mm.. * Line possibly due to siderite.

spacings and visually estimated intensities are given in Table 2 (Columns 1 and 2). Column 3 gives the data by Sudo[11], and Column 4, the data by Engelhardt[5]. The reflections of chlorite from Shōgasé (Fig. 1 and Table 1, Column 1) are fairly diffuse and some bands are shading on the side of smaller spacings. These characteristics may indicate a rather irregular structure. On the other hand, the reflections of "chamosite" from the Arakawa mine are moderately sharp. There is high similarity not only between the diagrams of chlorites from Shōgasé and from Arakawa, but also among them and those of "chamosite" from Schmiedefeld, Thuringia. These data bear some resemblances to those of ortho-hexagonal kaolin-type chamosite described by Brindley[1], but some discrepancies are found between them.

Engelhardt interpreted his "chamosite" data as a layer structure of chlorite cell with orthorhombic (ortho-hexagonal) instead of

monoclinic axes. Although the evidences for his interpretation were not satisfactory, the data described here can be thoroughly interpreted according to his idea of the "chamosite" cell. Thermal behaviours given in the next section are also in agreement with his idea.

The lattice parameters were estimated as follows: Basal reflections at 14.1, 7.05 and 3.53Å and their higher orders were used to obtain the c-parameters. The b-parameters were obtained by taking the strong 1.55Å reflections as the 060. The bases of the cells were assumed to be centred and ortho-hexagonal in shape, so that $a = b/\sqrt{3}$. The calculated spacings, with their *hkl* indices, are compared with the measured spacings in Table 2, Columns 1 and 2. The agreement is everywhere close. Some basal reflections with an odd number for *l* index are recorded. The cell dimensions obtained here are shown in Table 3, where they are compared with those given by Engelhardt[5].

Table 3. Cell dimensions of ortho-hexagonal iron-rich chlorites.

	1	2	3
a	$b/\sqrt{3}=5.38$Å	$b/\sqrt{3}=5.40$Å	5.393 kX
b	9.32	9.35	9.341
c	14.16	14.17	14.00

1. Chlorite from Shōgasé.
2. "Chamosite" from the Arakawa mine.
3. "Chamosite" from Schmiedefeld, Thuringia. Data by Engelhardt[5].

Thermal properties

Differential thermal analysis curve of chlorite from Shōgasé is given in Fig. 3. It has two endothermic peaks; at about 600°C, and about 730°C.

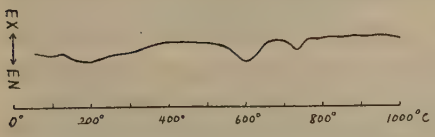

Fig. 3. Differential thermal analysis curve of chlorite from Shōgasé.

The X-ray diagrams of the material heated up to 670°C, the end of the first endothermic curve, show a strengthening of 14Å line and considerable weakening of the higher order lines.

These thermal behaviours are characterics tic to chlorite-type structure.

Note on the nomenclature

There are a number of mineral species belonging to the iron-rich chlorite; thuringite, chamosite, daphnite, bavalite, aphrosiderite, metachlorite, etc., and their nomenclatures are confused. But it has been shown that most of them except chamosite have similar structure.

The minerals hitherto called chamosite are generally found in the iron-rich sedimentary formations, and have been shown by Brindley[1] and others[4] to include kaolin-type and chlorite-type minerals; the common chamosite has kaolin-type layers, consisting of a mixture of monoclinic and ortho-hexagonal cells in varying proportions; several chamosites including the specimen of type locality have probably monoclinic cells like most of other chlorites; "chamosite" from Schmiedefeld, Thuringia already mentioned has been considered as to have an orthorhombic (ortho-hexagonal) cell based on the chlorite-type layer. The chlorites described here belong to the latter category. It has been stated by Brindley[1] and Hey[7] that these complex relations need a new nomenclature.

The chemical compositions of the Shōgasé chlorite and also "chamosites" from the Arakawa mine and Schmiedefeld are alike to earlier analyses of some of thuringites, chamosites as well as to some of aphrosiderites (Table 1). Chemically these three chlorites belong to thuringite, and the "chamosite", having the above-mentioned difficulties in nomenclature, must be abandoned*. Aphroside-

* After Dana's System 6th edition (1914, p. 658), chamosite is a variety of thuringite. The original sample of chamosite included siderite. It was reexamined later and shown to have a composition approximating thuringite.#

rite is used for more magnesia-rich members.

These chlorites have ortho-hexagonal cells, and their structural relation to thuringite is similar to that of ortho-antigorite to antigorite as studied by Brindley and Knorring[3].

For the reasons, these chlorites may be named "ortho-thuringite". But then, there arises a confusion with the term "orthochlorite". The writer prefers to leave this question of nomenclature unsettled at present.

In this sense, it is not reasonable to use the name "chamosite" as a mineral name. As suggested by Hey[7], it must be used as an inclusive term like limonite or wad.

Acknowledgements

The writer wishes to acknowledge to Prof. T. Yoshimura for his guidance and critically reading the manuscript and also to Lect. Y. Okamoto for the gift of samples. Thanks are due to Mr. N. Tanaka, Institute of Economic Geology, Kyushu University for the help in the thermal study. The writer also greatly indebted to Prof. T. Sudo, Tokyo University of Education, who offered the suggestions to his work. Finally, the writer should like to record his hearty thanks to Mr. Y. Kora and the staffs of Kurosaki Fire-brick Manufacturing Company for the understandings and encouragements during his incumbency and thereafter.

REFERENCES

1) Brindley, G. W.: Min. Mag., **29**, 502 (1951).
2) Brindley, G. W. and K. Robinson: X-ray identification and crystal structure of clay minerals, 173 (1951).

#The analyses of chamosite generally inform us of rather smaller Fe_2O_3 contents than thuringite. But the writer considers that the disparities are small and it is not necessary to distinguish these two species refered to their chemical composition.

3) Brindley, G. W. and O. von Knorring: Am. Miner., **39**, 794 (1954).
4) Caillere, S. and S. Henin: Clay Min. Bull., **1**, 134 (1951).
5) Engelhardt, W. von: Zs. Kr., **104**, 142 (1942).
6) Hallimond, A. F.: Min. Mag., **25**, 441 (1939).
7) Hey, M. H.: Min. Mag., **30**, 277 (1954).
8) Jung, H. and E. Köeler: Chem. Erd., **5**, 182 (1930).
9) Jung, H.: Chem. Erd., **6**, 275 (1931).
10) Orcel, J.: Bull. Soc. Fr. Min., **50**, 75 (1927).
11) Sudo, T.: Bull. Chem. Soc. Japan, **18**, 281 (1943).
12) Websky: Zs. Geol. Gesel., **31**, 212 (1879).

Manuscript received January 9, 1955.

MINERALOGICAL JOURNAL, VOL. 1, NO. 4, PP. 233-241, JUNE, 1955

ON THE STRUCTURAL VARIATIONS OF SOME JAPANESE KAOLINITES

SHINICHI IWAI

Mineralogical and Geological Department,
Tokyo Institute of Technology

ABSTRACT

Kaolinite crystals collected from several localities in Japan were examined in detail by means of X-ray powder technique, with the conclusion that there are marked structural variations in them.

Summarising the results so far obtained, these kaolinites were classified into three types on the basis of degree of crystallinity.

Type (1) Ordered type without randomness.

Type (2) Partially disordered type with some amounts of $\pm$ n $\frac{1}{3}\vec{b}$ random displacements.

Type (3) Partially disordered type with $\pm$n $\frac{1}{3}\vec{b}$ and some additional random displacements parallel to layers.

It is noteworthy that the degree of orderedness of the minerals is roughly correlated with their modes of occurrence and with their morphological appearances under the electron microscope.

Introduction

Numerous studies have hitherto been made concerning the so-called "stacking disorder" found in the layer structure of clay minerals.

The present writer[10),11)] has also contributed papers on the summarized feature of some kaolinites and halloysites from Japan. Since then, he has obtained a number of additional kaolinitic materials from various localities, and a detailed examination has been carried out on those specimens.

Throughout the course of this study, his attention was mainly concentrated upon the structural variations of these minerals, which

seemed to be correlated with their modes of occurrence. With the aid of X-ray diffraction patterns, particularly on the basis of the variation in the intensity and profile of each diffraction line, the writer classified these minerals into three types from the view-point of crystallinity.

Specimens and methods

Specimens used in this study are listed in Table 1.

Ina Clay (the sixteenth specimen) is composed of hydrated halloysite instead of kaolinite, but is quoted here to give the lowest limit of crystallinity of kaolinite structure.

Kaolinite crystals were separated from the crude clays by means of elutriation hand-picking, etc. Some kinds of purified materials contained a small amount of quartz grains, whose further removal was entirely impossible owing to their extremely small size. It seems that fine quartz grains are comparatively abundant in clays composed of kaolinite of lower crystallinity, though they are almost free in clays containing highly crystallized ones.

In order to obtain excellent resolution of diffraction lines, the powder specimens were made up into rods of 0.2~0.3 mm. in diameter with the aid of adhesive dextrine as the binding agent. The camera employed was of normal type with radius 2.84 cm. by which, using Cu radiation, we could record a comparatively long spacing up to 12 kX, with considerable resolving power by virtue of its sharp collimation system. Filtered Cu radiation at 20~25 kV., 6~8 mA., was used throughout this study.

All diffraction lines arising from kaolinite minerals showed clear continuous rings, even photographed without rotation. The powder specimens were, therefore, not rotated during exposure, which made it possible to distinguish kaolinite reflections from faint quartz ones superimposed on the former, since quartz reflections would appear in spotty patterns in such cases. But this technique was not always in

Table 1. Localities and mo

Specimens	Localities*	
1. Ibusuki Kaolin	Ibusuki-gun, Kagoshima Prefecture, Japan	Massive deposit
2. Kanpaku Kaolin	Kawachi-gun, Tochigi Prefecture, Japan	Vein deposit in
3. Hakusan Kaolin	China	A bed of Carbo
4. Zettlitz Kaolin	Czechoslovakia	
5. Georgia Kaolin	U. S. A.	A bed of Upper
6. Ibusuki Kaolin	The same as 1 but from a different part	
7. Hongkong Kaolin	China	
8. Takatama Kaolin	Adachi-gun, Fukushima Prefecture, Japan	A hydrothermal
9. Naegi Kaolin	Ena-gun, Gifu Prefecture, Japan	Crystals embedd
10. Iwate Kaolin	Shimohei-gun, Iwate Prefecture, Japan	A Tertiary bed
11. Motoyama Kibushi-Clay	Seto, Aichi Prefecture, Japan	A Tertiary bed
12. Oohata Kibushi-Clay	Aichi-gun, Aichi Prefecture, Japan	
13. Tokiguchi Gaerome-Clay	Toki-gun, Gifu Prefecture, Japan	
14. Hagishou Clay	Nishiiwai-gun, Iwate Prefecture, Japan	A Tertiary bed
15. Tsukinokawa Clay	Kitamatsuura-gun, Nagasaki Prefecture, Japan	Weathered volca
16. Ina Clay (dried at 150°C)	Kamiina-gun, Nagano Prefecture, Japan	

* 1, 6. 鹿児島県揖宿郡指宿鉱山
2. 栃木県河内郡関白鉱山
8. 福島県安達郡
9. 岐阜県惠那郡苗木町
10. 岩手県下閉伊郡岩手炭坑
11. 愛知県瀬戸市郊外
12. 愛知県愛知郡保見村大畑
13. 岐阜県土岐郡土岐津町
14.
15.
16.

of occurrence of specimens.

ies of occurrence[9]	Morphological appearance under electron microscope[8][9][11]
hydrothermally altered andesite.	Distinctly platy, hexagonal shape.
drothermally altered liparite.	,,
ous formation with coal seams.	
	Distinctly platy, hexagonal shape.
taceous formation with coal seams.	,,
	,,
	Pipe-like shape.
l vein.	,,
n a Tertiary clay bed.	Thin platy irregular shape.
ciated with coal seams.	,,
ciated with lignite seams.	,,
,,	,,
,,	,,
ciated with lignite seams.	,,
ash.	Complicated polyhedron.
,,	,,

県西磐井郡荻荘村
県北松浦郡
県上伊那郡伊那町

Table 2. Inter-layer spacings of Japanese kaolinites.

Indices†	1		2		3		4		5		6		Indices†	7		8		9		10		11		12		Indices†	13		14		15		16	
	d(kX)	Int.	d(kX)	Int.	d(kX)	Int.	d(kX)	Int.	d(kX)	Int.	d(kX)	Int.		d(kX)	Int.	d(kX)	Int.	d(kX)	Int.	d(kX)	Int.	d(kX)	Int	d(kX)	Int.		d(kX)	Int.	d(kX)	Int	d(kX)	Int.	d(kX)	Int.
														10.0**	w														10.1**	ww	9.9**	ms		
001	7.12	ss	7.12	ss	7.12	ss	7.12	ss	7.12	ss	7.12	ss	001	7.12	ss	7.24	ss	7.12	ss	7.12	ss	7.12	ss	7.12	ss	001	7.2	ss	7.3	s	7.4	s	7.4	s. b
	5.72	w																															
	4.85	w																															
020	4.40	s	4.44	s	4.44	w	4.44	w	4.44	s	4.45	s	02, 11	4.43	ss	4.45	s	4.45	s	4.45	ms	4.45	s	4.45	s	02, 11	4.39	s	4.43	s. b	4.42	ss. b	4.44	ss
$1\bar{1}0$					4.38	s	4.38	s	4.36	s	4.34	s	110					4.37	mw	4.34	s													
$11\bar{1}$, $1\bar{1}\bar{1}$	4.16	ms	4.12	m	4.12	ms	4.12	m	4.09	m	4.16	m	$11\bar{1}$	4.19	w	4.12*	w	4.18	m	4.09	w	4.25*	m	4.10*	s		4.08	ww	4.27*	m	4.14	w		
$02\bar{1}$, 021	3.83	mw	3.83	w	3.82	w. b	3.86	w	3.83	w	4.01	ww		3.83	www	3.89	ww	3.86	w	3.80	w										3.89	ww		
002	3.56	ss	3.56	ss	3.56	ss	3.56	ss	3.56	ss	3.56	ss	002	3.54	s	3.56	s	3.56	s	3.53	ss	3.56	ss	3.56	ss	002	3.56	s	3.55	ms. b	3.52	s. b	3.60	ms. b
111	3.36	w	3.34	ww	3.37	w	3.31*	mw	3.34	w				3.32	ww	3.31	m	3.39	ww	3.32*	w	3.34*	m	3.31*	s		3.35	w	3.33*	s	3.32**	ww		
$11\bar{2}$, $1\bar{1}\bar{2}$	3.10	ww	3.10	ww	3.09	www	3.12	mw	3.10	ww								3.10	ww														
	2.95	m							2.82	www	2.82	ww				2.91	w																
022	2.73	w	2.70	w	2.72	ww	2.71	ww	2.72	ww								2.66	ww. b														
$20\bar{1}$, $13\bar{0}$, 130	2.56	m	2.53	ms	2.53	m	2.53	ms	2.57	mw	2.55	m	$20\bar{1}$, 130	2.54	m	2.55	m	2.55	m	2.54	m	2.57	m	2.56	ms. b	13, 20	2.54	m	2.56	m	2.56	m	2.56	m. b
$13\bar{1}$, 200, 112	2.48	ms	2.46	mw	2.46	m	2.46	m	2.47	m	2.48	ms	$13\bar{1}$, 200	2.48	mw	2.48	mw	2.47	mw	2.48	mw	2.50	m	2.46	w		2.48	w	2.49	w	2.48	w		
003	2.38	www	2.34	ww					2.37	w	2.37	w	003	2.38	ww	2.38	ww	2.38	ww	2.38	ww	2.38	ww	2.38	w	003	2.39	ms	2.34	m				
$20\bar{2}$, $13\bar{1}$	2.32	s	2.31	s	2.31	s	2.31	s	2.32	s	2.32	s	$20\bar{3}$, $13\bar{1}$	2.33	ms	2.33	ms	2.32	ms	2.32	ms	2.34	m	2.33	mw		2.30	w	2.28	w	2.34	ms	2.33	mw
$11\bar{3}$, 131	2.28	w	2.28	w	2.27	mw	2.26	w	2.28	mw	2.27	mw	$13\bar{2}$, 201	2.25	mw	2.28	w	2.30	w	2.27	w	2.29	w	2.28	w								
201, $13\bar{2}$, $23\bar{0}$	2.19	w. b	2.19	mw. b	2.18	w. b	2.18	w. b	2.17	w	2.18	w. b		2.17	www	2.18	w. b	2.14	ww	2.18	ww	2.12*	ww	2.17	w	04, 22	2.21	ww	2.12*	ww				
$02\bar{3}$, 041	2.11	ww	2.10	ww																													
023, $22\bar{2}$	2.06	ww	2.08	ww	2.04	ww	2.06	ww	2.04	ww	2.05	ww		2.05	ww					2.07	www												
$20\bar{3}$, $13\bar{2}$	1.980	m	1.980	mw	1.980	m	1.980	ms	1.982	mw	1.980	mw	$20\bar{3}$, 132	1.980	mw	1.982	mw	1.989	mw	1.980	mw	1.99	w	1.98	m. b		1.98	w	1.98	w. b	1.99	ww. b	2.01	ww. b
221, 132	1.933	ww	1.933	ww	1.932	www	1.923	ww	1.933	w	1.933	ww		1.938	ww																		
113, $13\bar{3}$	1.887	w	1.878	ww	1.883	w							$13\bar{3}$, 202			1.887	ww			1.883	ww	1.90	w	1.89	ww		1.89	www			1.89	w		
$15\bar{3}$, 202, $22\bar{3}$	1.828	w	1.826	w	1.828	w	1.817	ww	1.829	w	1.833	w		1.834	ww			1.837	ww			1.81*	ww	1.81	w	004			1.81	w			1.82	w
004	1.774	w. b	1.774	mw	1.772	w	1.772	w	1.774	w	1.780	w	004	1.783	w			1.781	w	1.772	w	1.79	www				1.78	ww						
150, $24\bar{1}$, $31\bar{1}$	1.738	ww			1.670	w	1.668	ww	1.673	ww	1.674	ww	$20\bar{4}$, 133	1.678	w	1.673	w	1.670	mw. b	1.690	ww	1.67	m	1.66	ms	31, 15, 24	1.67	m	1.68	mw	1.67	mw. b	1.68	w
$24\bar{0}$, $20\bar{4}$, $13\bar{3}$	1.658	s. b	1.651	s. b	1.652	w	1.651	ms.	1.653	ms	1.660	ms. b		1.651	m	1.651	mw			1.653	mw												
$24\bar{5}$, 133, 310	1.613	w	1.613	mw	1.613	w	1.607	w	1.618	w	1.618	w		1.618	w	1.613	ww	1.612	ww	1.623	www	1.62	ww	1.61	ww. b		1.61	www	1.60					
$15\bar{2}$, $13\bar{4}$	1.582	ww	1.567	ww	1.576	ww	1.576	ww	1.574	ww	1.567	ww		1.573	www			1.578	ww														
241, 114, $13\bar{4}$	1.539	w. b	1.532	mw	1.530	w	1.530	w	1.542	w	1.537	w. b	$13\bar{4}$, 203	1.532	w. b	1.537*	w	1.523	w. b	1.523	ww	1.54*	w	1.54*	w		1.53	ww	1.54*	w	1.54	w. b	1.53	ww
060, 331, 331	1.483	s	1.481	s	1.480	s	1.480	s	1.486	s	1.488	s	060, 331	1.483	ms	1.483	ms	1.488	m	1.486	ms	1.49	s	1.49	s	06, 33	1.49	s	1.49	s	1.48	s. b	1.48	ms. b
$33\bar{2}$, 061, etc.	1.452	w. b	1.445	w	1.453	ww. b	1.453	ww. b	1.453	w	1.453	ww. b	$33\bar{2}$, 061, 330	1.453	w	1.457	ww	1.453	ww	1.461	ww	1.46	ww	1.46	ww		1.45	ww	1.46	ww				
005					1.447	w	1.426	www	1.424	ww			005	1.428	www					1.424	ww												
	1.393	ww			1.394	ww																											
			1.383	ww	1.383	ww	1.387	www	1.382	ww	1.390	www	$33\bar{3}$, 062, $33\bar{1}$	1.373	ww	1.393	ww	1.394	ww			1.37	w	1.37	mw. b								
	1.368	ww	1.360	ww	1.360	ww	1.358	ww	1.360	ww	1.365	www		1.352	ww	1.364	ww			1.850	www								1.37*	w	1.36	ww		
	1.332	w. b	1.327	w	1.313	w	1.330	w	1.332	w	1.336	w	$13\bar{5}$	1.332	w	1.330	ww	1.332	ww	1.328	www	1.31	w	1.33	ww								
	1.307	w	1.300	mw	1.300	w	1.297	mw. b	1.300	mw	1.302	w. b	204	1.302	w	1.307	ww	1.307	w	1.297	ww												
	1.280	w	1.274	mw	1.292	w	1.274	w	1.279	w	1.277	w	$26\bar{1}$, $40\bar{1}$	1.280	w. b	1.277	w	1.277	w	1.280	w	1.28	w	1.28	w. b		1.28	w	1.28	w. b	1.28	w	1.28	w. b
	1.259	w			1.260	www			1.256	ww				1.257	ww																		
	1.238	w							1.241	ww	1.230	www																				
	1.228	mw	1.226	m. b	1.232	mw	1.233	mw. b	1.227	w	1.227	w				1.232	w	1.237	w	1.232	w	1.23	w	1.24	w		1.23	w	1.23	w. b	1.23	w. b	1.23	w. b

1. Ibusuki Kaolin, Japan.
2. Kanpaku Kaolin, Japan.
3. Hakusan Clay, China.
4. Zettlitz Kaolin, Czechoslovakia.
5. Georgia Kaolin, U. S. A.
6. Ibusuki Kaolin, Japan.
7. Hongkong Kaolin, China.
8. Takatama Kaolin, Japan.
9. Naegi Kaolin, Japan
10. Iwate Clay, Japan
11. Motoyama Kibushi-Clay, Japan.
12. Ochata Kibushi-Clay, Japan.
13. Tokiguchi Gaerome-Clay, Japan.
14. Hagishou Clay, Japan.
15. Tsukinokawa Clay, Japan.
16. Ina Clay (heat treated), Japan.

† Indices were rearranged after G. W. Brindley.
* Line due to quartz.
** Line due to hydrated halloysite.
Intensity sequence; ss, s, ms, m, mw, w, ww, www, b: broad line.

success, especially in the case that quartz existed in quantity.

A Geiger-counter X-ray diffractometer* was used to examine some details of diffraction patterns of four reference specimens which were supposed to represent typical types as to the degree of crystallinity.

Experimental

Table 2 illustrates the observed interplanar spacings and visually estimated relative intensities.

It is to be pointed out that the intensities of diffuse lines may be underestimated owing to broadness.

These photographs clearly show that some specimens give merely sharp lines, while the others give less number of sharp lines and broad ones accompanied with diffuse bands. Judging from the co-existence of sharp and diffuse lines, it is quite conceivable that the line broadening is not ascribable to small crystal size. Therefore, keeping in mind the number of lines and the sharpness of reflections, the writer classified the X-ray powder diagrams of various specimens as arranged in Table 2. In Table 2, the specimen with the largest number of sharp lines is found in the left column, and towards right, those with smaller number of lines, most of which are broad. All the reflections were indexed after the results published by G. W. Brindley et. al.[1] In Fig. 1, two types of reflections, one of which is of $k \neq 3n$ (n is an integer) and the other of $k=3n$, are schematically represented. As can be seen in this diagram, from the top towards the bottom, the reflections of the $k \neq 3n$ type (left side) gradually decrease both in number and in intensity. This is also the case with the $k=3n$ type, though not so markedly as with the former.

In Fig. 2 powder reflections obtained in the range of $10° \sim 15°$ (θ) with four specimens were arranged from an ordered type top to less ordered types (towards the bottom).

* This apparatus[7] was constructed in our laboratory with the co-operation of M. Nakahira of the Scientific Research Institute.

Fig. 1. Diagramatic representation of intensity variation.

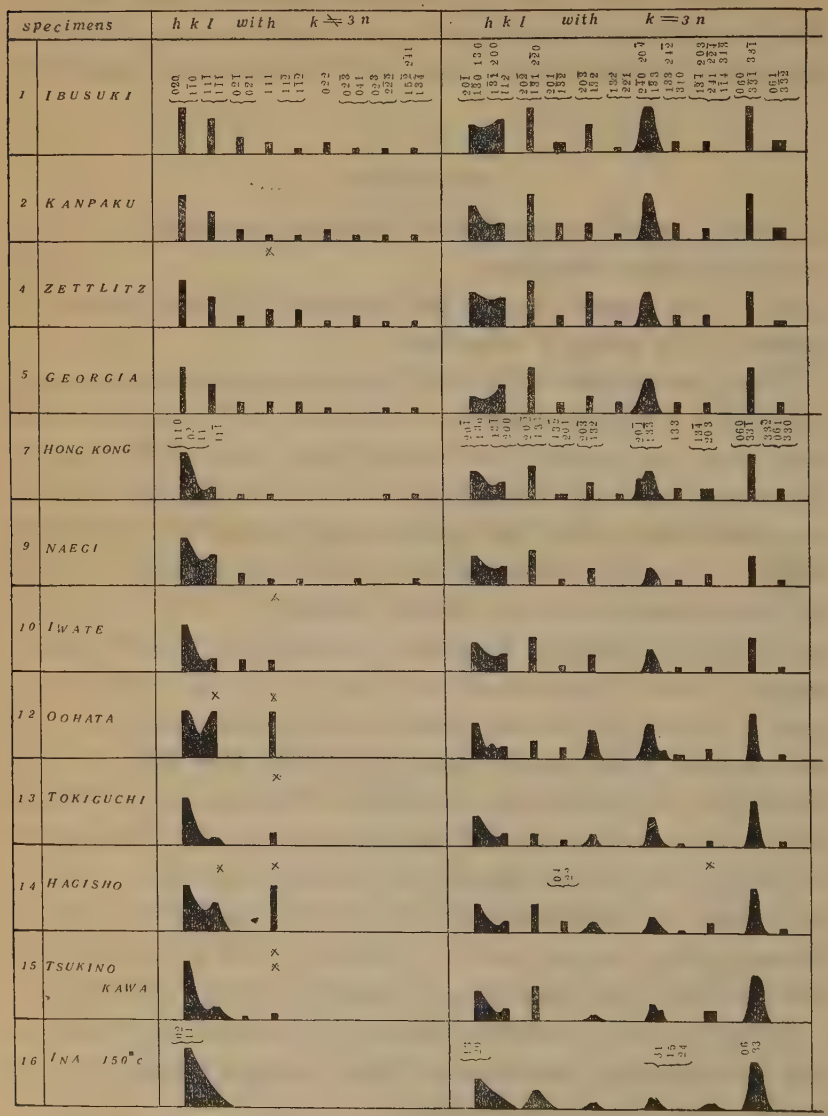

※ Lines due to quartz. ※※ Lines due to hydrated halloysite.

1~5: Type (1), 7~12: Type (2), 13~16: Type (3).

As revealed from Table 2 and Fig. 1, the specimens can be classified into three types, based on the characteristic features of diffraction patterns:

Type (1). Ibusuki~Georgia

($00l$): sharp

(hkl): generally sharp

Type (2). Hongkong~Oohata

($00l$): broader than those of type (1)

(hkl) k=3n: still sharp

$k\neq$3n: often diffuse or weak and some of them disappeared.

(020): mixed with two-dimensional tailed bands, which is obviously seen in those line profiles of Takatama Kaolin and Motoyama Kibushi-Clay in Fig. 2.

Type (3). Tokiguchi~Ina (dried at 150°C)

($00l$): remarkably broad and the (001) spacing expands to 7.3~7.4 kX., occasionally accompanied with a line, d=10 kX (due to hydrated halloysite).

(hkl) k=3n: markedly diffuse or vanished,

$k\neq$3n: almost unobservable.

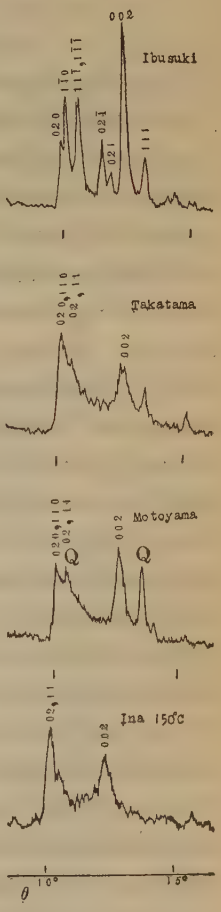

Fig. 2. Reproduced portion of X-ray diffractometer charts of four representative specimens.
Q: lines due to quartz.
X-ray: Ni-filtered Cu $K\alpha$ radiation at 25~30 kV., 15 mA., Scanning velocity: $\frac{1}{8}$° per minute, time const.: 4.8 secs., scale factor: 4, chart driving speed: 200 mm. per hour.

(020): having a tendency of the typical tailed reflection of two-dimensional type. Ina Clay in Fig. 2 shows this typical case.

From Table 1 and 2, the correlation between the diffraction feature, the mode of occurrence and the morphological appearance under the electron microscope can be summarized as in Table 3.

Discussion

The basic crystal structure of kaolinite has been investigated by J. Gruner[4], S. B. Hendricks[5] and G. W. Brindley[2]. In kaolinite, as have been pointed out by many workers[3), 6), 10)], in addition to the unique triclinic structure, there exist several varieties owing to the random stacking of unit structural layer, $Al_2Si_2O_5(OH)_4$.

The interactions between each layer are considered to be mainly due to the hydrogen bridges between oxygen atoms of one layer and hydroxyl groups of the adjacent. If these are the sole interactions between the layers, the random displacements of $\pm n\frac{1}{3}\vec{b}$ of one layer with regard to the others can freely take place, because the arrangement of O and OH atoms in the layers is of hexagonal type and the mutual displacements mentioned above do not alter the arrangement of these hydrogen bonds. On the other hand, if there exist any other interactions between the layers, it is quite probable that the stacking of layers are affected by these interactions, thus giving the crystal the tendency of taking a preferred structure as in the case with some of the kaolinite specimens.

In the X-ray diffraction patterns, the random shifts of $\pm n\frac{1}{3}\vec{b}$ do not affect the (*hkl*)-reflections with $k=3n$ but give rise to the diffusing of the reflections with $k\neq 3n$. In the reciprocal lattice representation, the lattice points with $k=3n$ are sharp, while those of $k\neq 3n$ spread in the direction of c*, the degree of the spreading depending upon the frequency of the occurrence of such mistakes.

Thus, if a specimen consists of crystals which are fully-disordered

with $\pm n\frac{1}{3}\vec{b}$ displacements, its diffraction lines of (*hkl*) will be the mixture of (*hk*) tailed reflections with $k \neq 3n$ and the three-dimensional sharp reflections with $k=3n$. On the other hand, if it consists of crystals which are partially disordered with random $\pm n\frac{1}{3}\vec{b}$ displacements, the (*hkl*) lines will be the mixture of broad (*hkl*) lines with $k \neq 3n$ occasionally accompanied with (*hk*) tailed reflections, and sharp ones with $k=3n$. The author is of opinion that the specimens classified under Type (2) have this latter type of randomness. It is to be noted that, in the sixteen specimens examined, no such specimen is found as representing the former type of randomness. If the specimen consisting of crystals partially disordered type with $\pm n\frac{1}{3}\vec{b}$ displacements accompanied with other kinds of mistakes, the reflections with $k=3n$ will also become diffuse. Furthermore, if the degree of disorder becomes more remarkable, the nature of diffraction pattern approaches to that of the so-called random layer lattice. The author considers that the specimens classified as Type (3) represent this case.

It appears that the crystals with increasing randomness hold a small amount of water molecules between the layers. The presence of the water causes a slight expansion of the inter-layer spacing. If a crystallite is built up with the random stratification of layers of 7.1 and 7.4 kX in thickness, the observable basal spacing will be a statistical mean of these two. Here, 7.1 kX corresponds to the thickness of a layer without water molecule and 7.4 kX to that with a small amount of water molecules. As can be seen in Table 2, this effect of random stratification is observable in the vicinity of 7.1 and 7.4 kX with (001) reflection, while, as the difference between 3.6 and 3.7 kX is rather small, this can not clearly be detectable with (002) reflection.

Thus, three types of Japanese kaolinites above mentioned are classified from their structures as follows:

Type (1): Ordered type, without random displacements.

Type (2): Partially disordered type, with $\pm n\frac{1}{3}\vec{b}$ random

displacements.

Type (3): Partially disordered type with $\pm n\frac{1}{3}\vec{b}$ and other kinds of displacements approaching to the so-called random layer lattice.

According to the modes of occurrence, these kaolinites can be grouped into two kinds; of hydrothermal origin and of sedimentary type. In the former, the well ordered crystals of type (1) (for instance Ibusuki, Kanpaku etc.) have distinctly platy habit, while the partially disordered crystals of Type (2) (for instance, Takatama) are of pipe-like shape. In the latter, the well ordered crystals (for instance, Georgia) are also of distinctly platy shape, while the partially disordered crystals of Type (3) are of thin irregular or complicated polyhedra. It seems that the shape of these partially disordered crystals becomes more and more indistinct with the increasing degree of disorder in the structures. These relations are summarized in Table 3.

Table 3. Correlation between the diffraction features, the modes of occurrence and the morphological appearances under the electron microscope.

Diffraction feature	Mode of occurrence	Morphology
Type (1)	hydrothermal vein or in old sedimentary beds	platy
Type (2)	hydrothermal vein or in Tertiary beds	pipe-like or thin irregular shape
Type (3)	weathered volcanic ash	irregular polyhedra

The writer wishes to express his sincere thanks to Dr. Hisao Yamada of this Institute for his interest in and criticism of this work and to Dr. Mitsuoki Nakahira of the Scientific Research Institute for valuable discussions. His thanks are also due to Mr. Yasuhiro Kuroda and Mr. Joyo Ossaka for their assistance in carrying out the experiments.

REFERENCES

1) Brindley, G. W.: X-ray Identification and Crystal Structure of Clay Minerals (Miner. Soc.), (1951).
2) Brindley, G. W. and K. Robinson: Min. Mag., **27**, 242 (1946).
3) Brindley, G. W. and K. Robinson: Trans. Farad. Soc., **42B**, 198 (1946).
4) Gruner, J. W.: Zeit. f. Krist., **83**, 75 (1932).
5) Hendricks, S. B.: Zeit. f. Krist., **95**, 247 (1936).
6) Hendricks, S. B.: Phys. Rev., **57**, 448 (1940).
7) Iwai, S., Y. Kagami and K. Uchida: J. Ceram. Asso. Jap., **59**, 432 (1951). (In Japanese).
8) Kawashima, C.: Ceramic Raw Materials. Vol. **2**, 298 (1949). (In Japanese)
9) Muraoka, M.: Geol. Surv. Jap., Report No. 145, (1952). (In Japanese).
10) Nakahira, M. and S. Iwai: J. Sci. Research Inst., **44**, 79 (1949).
11) Nakahira, M., S. Iwai and A. Suzuki: J. Sci. Research Inst., **45**, 52 (1951).

Manuscript received January 20, 1955.

MINERALOGICAL JOURNAL, VOL. 1, NO. 4, PP. 242-249, JUNE, 1955

ON INESITE FROM RENDAIJI*

SHIN'ICHIRO TAKASU**

Mineralogical Institute, University of Tokyo

Several reports have been published on inesite from various localities in this country.[1)3)7)9)] In view of the fact, however, that detailed descriptions on the crystal have not yet been given, it will be worth while to undertake a further investigation of the substance.

Material

The material of the present study was from the Rendaiji mine, Shizuoka Prefecture, about two miles north of Shimoda Port in the Izu peninsula. The geologic formations around the mine consist of highly propilitized tuffite and andesite of the Miocene origin. Numerous manganese bearing gold-silver deposits run parallel to one another through the formations and are being (or have been worked) at several places. The following is the list of the minerals found in these deposits; quartz, manganese bearing calcite, rhodochrosite, psilomelane, pyrolusite, inesite, penwithite rhodonite, chalcopyrite, chalcosite, malachite, chrysocolla, argentite, native tellurium, tellurobismuthite, rickardite, sylvanite ?, calaverite ?, hessite, empressite and weissite ?.

Inesite is found in quartz-rhodonite veins penetrating through the gold-silver deposits between Sarukui and Kakehashi, and the specimens used in the present investigation are mainly the radial aggre-

---

* Read at the meeting of the Mineralogical Society of Japan held in Fukuoka on Oct. 31, 1954.

** Present address: Matsuda Research Laboratory, Tokyo Shibaura Electric Company, Sunamachi, Tokyo.

Table 1. Goniometric data*.

	Old**	New**	ρ_{obs}	ρ_{calc}***	φ_{obs}	φ_{calc}***	F#	R#	I#	n#
a	{100 / 100}	$\bar{1}01$	90°02′	90°00′	83°17′	82°35′	L	S	A	10
b	{010 / 0$\bar{1}$0}	010	90 00	90 00	0 00	0 00	M	W	B	10
c	001	001	43 00	43 21	79 50	80 24	S	M	A	4
d	0$\bar{1}$1	0$\bar{1}$1	56 14	56 14	141 36	141 32	M	W	B	2
M	{1$\bar{1}$0 / $\bar{1}$10}	$\bar{1}\bar{1}$1	90 05	90 00	121 16	120 34	M	M	A	7
e	$\bar{1}$01	100	42 49	42 42	264 55	265 05	M	M	A	3
g	201	$\bar{2}$03	78 05	77 55	82 50	82 05	S	M	A	2
f	210	$\bar{2}$12	89 53	90 00	64 30	64 15	S	M	A	1

* By zone adjustment.

** Old: indices after Dana.
New: indices after the present author.

*** After Dana's System of mineralogy. The set of constants is given by Scheibe.
a : b : c = 0.9753 : 1.0000 : 1.3208, $\alpha = 92°18'$, $\beta = 132°56'$, $\gamma = 93°51'$.

#F: development of faces. L: large, M: middle, S: small.
R: intensity of reflexion. S: strong, M: medium, W: weak.
I : clarity of image. A: good, B: poor.
n : number of measurement.

Table 2. Combination of faces.

	1	2	3	4	5	F
a	+	+	+	+	+	5
b	+	+	+	+	+	5
c	+		+	+	+	4
d	+		+			2
M	+	+	+	+		4
e	+			+	+	3
g	+				+	2
f	+					1
Fig.	1	—	2	3	4	

1: platy crystal, 2~5: prismatic crystals, F: frequency.

gates of fibrous pale pink crystals embedded in a compact mass of quartz and rhodonite from Kakehashi. Besides these radial aggregates small prismatic crystals, 1~5 mm. long and 0.1~0.5 mm. thick, are also found inside small druses, occasionally with platy crystals.

These crystals are colourless and transparent when they are fresh but gradually become white on exposure and finally they turn into dark brown probably owing to the formation of manganese oxides in the crystals.

Morphological and optical studies[2)8)]

The observation with a Goldshmidt's two circle goniometer revealed the presence of the faces as listed in Table 1 and illustrated in stereographic projection, Fig. 1. In Table 2 the combination of faces and the frequencies of their appearance on fine specimens are given. Figs. 2~5 show the crystal habits of those specimens. (All the faces were indexed in conformity with the lattice constants as given below.)

The optical properties of inesite[10)] measured on small cleavage pieces are:

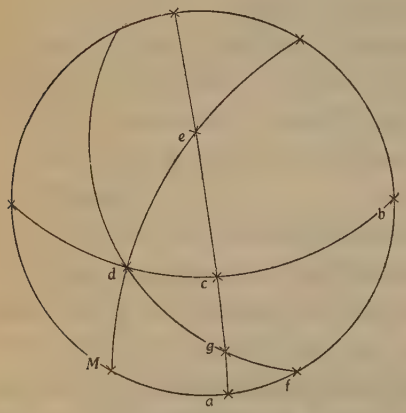

Fig. 1. Stereographic projection of inesite crystal.

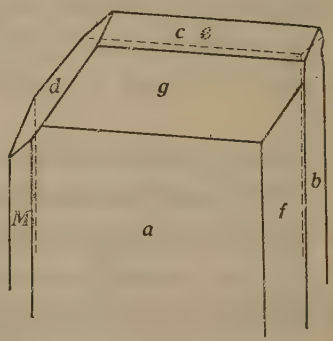

Fig. 2. Inesite from Rendaiji, with a platy habit.

n_1=1.62, n_2=1.64

and optically negative.

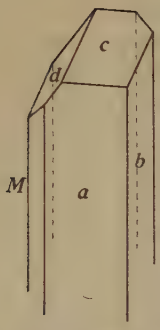

Fig. 3. Inesite from Rendaiji, with a prismatic habit.

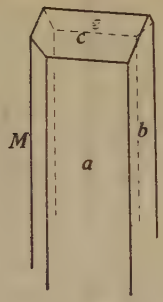

Fig. 4. Inesite from Rendaiji, with a prismatic habit.

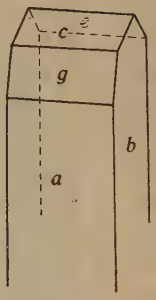

Fig. 5. Inesite from Rendaiji, with a prismatic habit.

Chemical analysis

A chemical analysis was carried out by H. Kaneko of the Research Laboratory, Nihon Denko Co.. The specimens were collected from the aggregates of the crystals in druses. The result is given in Table 3, together with the results obtained previously by other workers[6)7)8)].

The results of these independent analyses are in satisfactory agreement and lead the chemical composition of inesite to be $Mn_7Ca_2Si_{10}O_{28}(OH)_26H_2O$. The specific gravity was measured as 3.02.

X-ray diffraction data

The X-ray diffraction data with a Norelco X-ray spectrometer obtained of powdered specimens of prismatic crystals are shown in Table 4. Photographic method were also employed with a prismatic single crystal; a 90°-oscillation photograph and the zero, first and second layer Weissenberg photographs were taken about the c-axis.

Table 3. Chemical composition.

	1	2	3	4	5	6	Procedures of chemical analysis adopted by H. Kaneko
SiO_2	45.57%	44.99%	45.67%	44.50%	45.14%	44.71%	H_2SO_4 fume and HF treat
MnO	37.68	37.18	37.10	37.80	36.20	37.12	Volhard method
FeO			0.92				
Fe_2O_3				0.55	0.56	0.15	titration after amalgamation
CaO	8.53	8.40	9.33	7.86	6.98	7.31	oxalic acid method
MgO			0.86	0.27	0.37	0.42	oxine method
Al_2O_3				0.43	0.40	0.20	weighed in the form of phosphate
H_2O (total)	8.22	9.43	8.66	8.56	10.17	9.42	
$H_2O(+)$				4.90	9.58	6.12	ignition loss
$H_2O(-)$				3.66	0.59	3.30	loss below 110°C
Total	100.00	100.00	100.54	99.97	99.82	99.33	

1. Calculated value as $Mn_7Ca_2Si_{10}O_{28}(OH)_2 \cdot 5H_2O$.
2. Calculated value as $Mn_7Ca_2Si_{10}O_{28}(OH)_2 \cdot 6H_2O$.
3. By W. E. Richmond, from Quinault, Washington (1942).
4. By S. Tanaka, from Sarukui, Rendaiji (1930).
5. By Y. Okada, from Sarukui, Rendaiji (1931).
6. By H. Kaneko, from Kakehashi, Rendaiji (1952).

Table 4. X-ray powder data.

No.	I	2θ	Q-value $\times 10^4$	No.	I	2θ	Q-value $\times 10^4$
1	36	10.90°	(118)*	25	4	36.67°	1112
2	320	12.07	118	26	8	38.32	1150
3	32	16.96	232	27	52	38.69	1171
4	5	22.82	418	28	7	39.47	1217
5	8	22.99	424	29	5	39.85	1239
6	65	24.29	472	30	3	40.33	1268
7	9	25.26	510	31	11	41.45	1336
8	5	25.99	540	32	5	41.94	1367
9	8	26.21	549	33	5	42.99	1433
10	4	26.91	579	34	18	44.43	1526
11	4	27.03	583	35	8	44.70	1543
12	8	27.19	590	36	3	46.95	1560
13	6	27.30	594	37	4	47.32	1719
14	4	27.40	599	38	6	47.58	1737
15	58	27.94	622	39	3	48.25	1783
16	5	28.66	654	40	10	48.97	1830
17	4	29.18	677	41	12	52.42	2083
18	4	29.30	683	42	9	52.82	2111
19	5	29.47	690	43	7	61.50	2790
20	4	30.24	726	44	6	61.60	2801
21	9	34.40	930	45	5	62.86	2901
22	13	35.02	966	46	6	63.04	2917
23	12	35.99	1015	47	6	63.56	2960
24	6	36.85	1066				

With "Norelco" X-ray spectrometer, unfiltered Fe-radiation, slit: 1−0.006″ −1, scanning speed: 1°/min., scale factor: 4, multiplier: 1, time constant: 4 sec.. * By Fe $K\beta$ radiation.

The measurements on these photographs together with the X-ray spectrometer data gave as the lattice constants of the crystal the following values:

$$a_0=9.33\text{Å},\quad b_0=9.50\text{Å},\quad c_0=9.35\text{Å};$$
$$\alpha=94°09',\quad \beta=94°39',\quad \gamma=97°37'.$$

The unit cell chosen is the reduced one. These values are simply

related to those obtained by Richmond[8], the matrices of transformation[10] being given in Table 5.

Table 5. Transformation Matrices.

R→D-S	T→R	D-S→T	D-S→R	R→T	T→D-S
$\bar{1}\ 0\ \bar{1}$	$1\ 0\ 1$	$\bar{1}\ 0\ 0$	$\bar{1}\ 0\ \bar{1}$	$0\ 0\ \bar{1}$	$\bar{1}\ 0\ 0$
$0\ \bar{1}\ 0$	$0\ \bar{1}\ 0$	$0\ 1\ 0$	$0\ \bar{1}\ 0$	$0\ \bar{1}\ 0$	$0\ 1\ 0$
$1\ 0\ 0$	$\bar{1}\ 0\ 0$	$1\ 0\ 1$	$1\ 0\ 0$	$1\ 0\ 1$	$1\ 0\ 1$

D-S: Dana and Scheibe, R: Richmond, T: the present author.

The relation between the axial orientations given by Dana and Scheibe, Richmond and the present author is visualized in Fig. 6.

Use was made of the method of testing for piezo-electricity on small crystal with the apparatus constructed and described by Iitaka[4] of this labolatory and the result obtained was that the crystal is, though not strongly, definitely piezo-electric, thus leading to the conclusion that its space group is $P\bar{1}$.

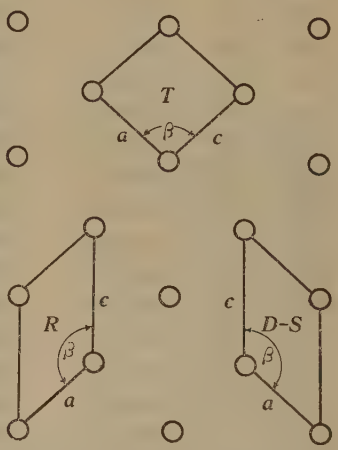

Fig. 6. The Relation between the unit cells adopted by Dana and Scheibe, Richmond and the present author. (a-c plane.)
D-S: Dana and Scheibe,
R: Richmond,
T: the present author.

The author wishes to express his sincere thanks to Prof. T. Ito, M.J.A. and Prof. N. Katayama for their suggestions and encouragements during the course of this work. His thanks are also due to Dr. R. Sadanaga, Dr. H. Minato, Dr. N. Morimoto, Mr. Y. Iitaka and Dr. K. Sakurai, for their help, and to Mr. H. Kaneko for putting the result of his chemical analysis at the author's disposal.

REFERENCES

1) Awazu, H.: Syumi no Kobutsu, 2, 19 (1930). (in Japanese)
2) Dana, E.S.: System of Mineralogy, 561 (1920).
3) Howells, E.R., D.C. Phillips and D. Rogers: Acta Cryst., 3, 210 (1950).
4) Iitaka, Y.: Acta Cryst., 6, 663 (1950).
5) Ito, T.: X-Ray Studies on Polymorphism, 189 (1950).
6) Kato, T.: Jour. Geol. Soc. Jap., 37, 35 (1930).
7) Okada, I.: Jour. Jap. Ass. Miner., Petr. & Econ. Geol., 5, 213 (1931). (in Japanese)
8) Richmond, W.E.: Amer. Miner., 27, 563 (1942).
9) Shibata, H.: Jour. Geol. Soc. Jap., 37, 181 (1930). (in Japanese)
10) International table of crystallography for the determination of crystal-structures (1953).

Manuscript received January 25, 1955.

MINERALOGICAL JOURNAL, VOL. 1, NO. 4, PP. 250-254, JUNE, 1955

SHORT COMMUNICATIONS

RECUEIL MINERALOGIQUE (III)

JUN ITO

Mineralogical Institute, University of Tokyo

(4) *Riebeckite from Sepori in the Fukushin-san district, Korea*

In the Fukushin-san district the regionally metamorphosed rocks of the Shogen System are widely distributed. They were intruded by an alkaline plutonic complex consisting of granites, quartz-syenites and alkaline-syenites. Riebeckite crystals are found in the pegmatitic pockets in granites that cropped out at Sepori* and are composed chiefly of quartz, microcline, biotite and riebeckite.

The crystals studied were separated from the rock specimens collected by Dr. A. Miyashiro by means of an electro-magnetic separator and Clerici solution. Under the microscope neither zonal structure nor inclusion were observed.

The optical properties are as follows: $\alpha=1.701$ $\gamma=1.711$ (by immersion method); pleochroism: X, Y blue, Z yellow.

X-Ray powder diffraction patterns with Cu $K\alpha$ radiation which were taken by a North American Philips Geiger Counter X-Ray diffractometer were indexed by comparing with the pattern of a Bolivian crocidorite[3] (I 2/m, $a_0=9.89$Å, $b_0=17.95$Å, $c_0=5.31$Å, $\beta=72°\frac{1}{2}'$). From the spacings (310), (330), (040), (002), (251) and (361) the cell dimensions of riebeckite from Sepori were obtained as follows: $a_0=9.69$Å, $b_0=18.09$Å, $c_0=5.34$Å, $\beta=72°11\frac{1}{2}'$. The measured 2θ and Q

* Sepori: (127°14'E 38°33'N), Central Korea, 細浦里.

values as well as calculated Q values from the constants obtained are given in Table 1.

Table 1. X-ray powder data of riebeckite from Sepori.
(Cu $K\alpha$ Ni fil., 1.5417Å)

No.	*hkl*	2θ	Q_{obs}	Q_{calc}	*I*
1	020	9°27′	0.0121	0.0122	m
2	110	10 31	0.0141	0.0141	v.s.
3	101	17 4	0.0370	0.0371	m
4	130	17 27	0.0387	0.0386	w
5	200	18 38	0.0440	0.0444	s
6	040	19 38	0.0489	0.0489	s
7	231	26 7	0.0858	0.0854	m
8	150	26 24	0.0877	0.0876	m
9	240	27 14	0.0933	0.0934	s
10	310	28 39	0.1030	0.1030	v.s.
11	321	29 55	0.1121	0.1131	m
12	330	31 57	0.1274	0.1275	v.s.
13	251	32 49	0.1343	0.1344	s
14	$\bar{2}31$	32 54	0.1349	0.1357	s
15	202	34 22	0.1468	0.1486	m
16	161	34 26	0.1473	0.1473	m
17	002	35 16	0.1545	0.1545	s
18	350	37 39	0.1753	0.1764	m
19	$\bar{2}51$	38 38	0.1841	0.1847	m
20	361	41 25	0.2107	0.2110	m
21	0,10,0	50 18	0.3044	0.3060	m
22	1,11,0	56 51	0.3820	0.3813	m
23	480	56 14	0.3746	0.3736	m
24	600	58 20	0.4004	0.3999	m

$a^{*2}=0.0111$, $b^{*2}=0.0306$, $c^{*2}=0.03863$, $2a^*c^*\cos\beta^*=0.01258$.

Chemical composition of riebeckite analyzed by the author is given in Table 2. The specific gravity obtained by means of the picnometer method is 3.39 (18°C). The density, derived from the chemical composition and the unit cell dimensions is 3.47 and is rather higher than the measured value.

Table 2. Chemical analysis of riebeckite from Sepori. (Analyst: J. Ito).

	Weight percentage	Molecular proportions	Oxygen atoms	Atomic ratios	Atomic ratios on basis 24 (O, OH, F)	
SiO_2	49.82%	0.829	1.658	0.829	7.685	7.880
TiO_2	0.90	0.011	0.022	0.011	0.102	
Al_2O_3	0.51	0.005	0.015	0.010	0.093	
Fe_2O_3	16.57	0.104	0.312	0.208	1.928	5.024
FeO	21.53	0.300	0.300	0.300	2.781	
MnO	0.53	0.007	0.007	0.007	0.065	
MgO	1.09	0.027	0.027	0.027	0.250	
CaO	0.76	0.014	0.014	0.014	0.130	2.187
Na_2O	6.54	0.105	0.103	0.210	1.946	
K_2O	0.57	0.006	0.006	0.012	0.111	
H_2O	2.03	0.112	0.112	0.224	2.076	2.289
F	0.45	0.023	0.011	0.023	0.213	
$F=O_2$	−0.21					
Total	101.09%		2.589		$\left(\frac{24}{2.589}=9.270\right)$	

Riebeckite from Sepori may be expressed by the formula:

$(OH, F)_{2.289}$ $(Ca, Na, K)_{2.187}$ $(Mg, Mn, Fe^{2+}, Fe^{3+})_{5.024}$ $(Ti, Al, Si)_{7.880}$ $O_{21.711}$

(5) *Aegirine from Hoansan,* in the Fukushin-san district, Korea*

The quartz syenites of eastern Fukushin-san, are composed of aegirine, riebeckite, quartz, microcline, albite and small amounts of zircon. Riebeckite has already been studied by Miss Tami Inoue[1]. The present author studied mineralogically the aegirine from Hoansan which was collected by Dr. A. Miyashiro**. The sample for chemical analysis was separated by means of electro-magnetic separator and Clerici solution.

Under the microscope it is strongly pleochroic; X and Y yellowish green, Z brownish yellow; and the zonal structure is not found.

* Hoansan: (127°10′E, 38°31′N), Central Korea, 虎岩山.
** A. Miyashiro: Geological Institute, University of Tokyo.

The specimens are not suitable for study of the crystal morphology.

X-ray powder patterns (with Cu $K\alpha$ radiation), using a North American Philips Geiger Counter X-ray Diffractometer, were obtained to calculate the cell dimension of aegirine. Each reflection was indexed with the aid of the known unit cell dimensions of clinopyroxene[2]. To calculate the cell constants of aegirine from Hoansan

Table 3. X-ray powder data of aegirine from Hoansan.
(Cu $K\alpha$, Ni fil., 1.54178Å)

No.	*hkl*	2θ	Q_{obs}	Q_{calc}	*I*
1	110	13°55′	0.0247	0.0246	s
2	200	19 13	0.0469	0.0470	m
3	020	20 7	0.0514	0.0515	s
4	220	28 1	0.0986	0.0986	s
5	221	29 58	0.1125	0.1132	s
6	310	30 49	0.1187	0.1186	v.s.
7	131	35 20	0.1556	0.1555	m
8	202	35 38	0.1576	0.1579	m
9	002	36 17	0.1632	0.1632	s
10	330	42 34	0.2220	0.2218	s
11	331	42 38	0.2228	0.2233	s
12	421	43 9	0.2279	0.2280	m
13	420	43 14	0.2288	0.2396	m
14	402	44 53	0.2456	0.2466	m
15	$20\bar{2}$	46 29	0.2624	0.2625	w
16	602	46 55	0.2670	0.2661	w
17	$42\bar{1}$	52 50	0.3337	0.3326	s
18	150	52 57	0.3349	0.3340	s
19	531	57 7	0.3853	0.3852	s
20	440	57 52	0.3945	0.3942	v.s.
21	600	60 13	0.4241	0.4230	s
22	350	60 37	0.4293	0.4280	s
23	602 $40\bar{2}$	61 47	0.4443	0.4294 0.4558	m
24	060	63 23	0.4651	0.4640	m
25	$53\bar{1}$	67 5	0.5146	0.5159	s

$a^{*2}=0.01175$, $b^{*2}=0.01289$, $c^{*2}=0.04080$, $2a^*c^*\cos\beta^*=0.01307$.

the reflections for ten planes (220), (310), (440), (200), (002), (020), (531), (53$\bar{1}$), (421) and (42$\bar{1}$) were used. The results are as follows: a_0=9.67Å, b_0=8.81Å, c_0=5.19Å, β=72°38′. The measured 2θ and Q values and calculated Q values from the constants estimated are given in Table 3.

Chemical composition of aegirine from Hoansan analyzed by the author are shown in Table 4.

Table 4. Chemical composition of aegirine from Hoansan. (Analyst: J. Ito.)

	Weight percentage	Molecular proportions	Oxygen atoms	Atomic ratios	Atomic ratios on basis 6(O)	
SiO_2	50.17%	0.835	1.670	0.835	1.958	2.00
Al_2O_3	0.93	0.009	0.027	0.018	0.041	
TiO_2	0.57	0.007	0.014	0.007	0.016	1.03
Fe_2O_3	31.14	0.195	0.585	0.390	0.918	
FeO	2.27	0.032	0.032	0.032	0.074	
MnO	0.58	0.008	0.008	0.008	0.018	
MgO	0.19	0.004	0.004	0.004	0.009	
CaO	1.24	0.022	0.022	0.022	0.051	0.97
Na_2O	12.07	0.195	0.195	0.390	0.918	
K_2O	tr.					
Ign. L.	0.52					
Total	99.68%		2.557		$\left(\frac{6}{2.557}=2.345\right)$	

Aegirine from Hoansan may be expressed by the formula:

$(Na, Ca)_{0.97}$ $(Mg, Mn, Fe^{2+}, Fe^{3+}, Ti)_{1.03}$ $(Al, Si)_{2.00}$ $O_{6.00}$.

The optical properties are as follows: α=1.754, γ=1.805, 2V(−) =60°–66°. The calculated density derived from the unit cell dimension (3.618) is rather higher than the measured value (3.56) determined by means of picnometer method.

References

1) Inoue, T.: Bull. Geol. Soc. Jap., 56, 71 (1950).
2) Kuno, H. and H. H. Hess: Am. Jour. Sci., 251, 741 (1953).
3) Whittaker, E. J.: Acta Cryst., 2, 321 (1949).

Contents of "KOBUTSUGAKU ZASSHI,"

Journal of the Mineralogical Society of Japan

in Japanese

VOL. 2, No. 2 (January, 1955)

Original Articles

Some Considerations of Differential Thermal Analysis Curves.....
.....K. Nagasawa and Y. Tsuzuki... 93
Diagrams for Determining Orientation of Thin Sections of Pyroxene and Amphibole.....T. Sueno...104
Ganophyllites from Ananai Mine, Kochi Prefecture and from Ozu Mine, Ehime Prefecture.....T. Yoshimura, H. Shirozu and F. Hirowatari...108
Stilpnomelane from the Skarn of Obira Mine, Oita Prefecture .....
.....H. Shirozu....115
On Jarosite and its Occurrence from Tearai Hot Spring, Kirishima Volcano
..... K. Kinoshita, K. Muta, H. Minato and Y. Takano...121

Short Communications

Communications on Minerals of Japan (Part 6).....Mumeikai Group...130
13. Euxenite-Polyclase from Ishikawa District, Fukushima Prefecture
..... K. Sakurai
14. Euxenite-Polyclase from Nogita, Fukuoka Prefecture.....
.....Y. Okamoto and K. Sakurai
15. Euxenite from Tsukumoushi, Iwate Prefecture.....
.....O. Nagashima and K. Sakurai
16. Dolomite from Igashima Mine, Niigata Prefecture..... S. Takasu

Reviews

Some Memoirs of My Stay in England .....R. Sadanaga...139

Proceedings 153

Contents of "KOBUTSUGAKU ZASSHI,"

Journal of the Mineralogical Society of Japan

in Japanese

VOL. 2, NO. 3 (May, 1955)

Memorial of Shukusuke Kōzu .....J. Harada. front.

Original Articles

Structural Changes of Schiller-Feldspar due to the Heat Treatment (I)
.....T. Tomisaka and G. Shibuya...155

Lepidocrocite from the Abeshiro Mine, Aomori Prefecture.....
..... T. Takeuchi and M. Nambu...165

On the Pyromorphite-Mimetite Series found in Japan.....
.....T. Ishimori, H. Waki and K. Muta...172

Zeunerite from Miyoshi Mine, Okayama Prefecture .....K. Henmi...182

Contact Metamorphism of Serpentine by Pegmatite at the Kyuragimachi, Saga Prefecture .....K. Muta...187

Short Communications

Dielectric Dispersion of Low Quartz.....
..... R. Kiriyama, H. Ibamoto, M. Koizumi and R. Kitagaki...200

Specularite from Ayumukotan, Mashike Town, Teshio Province, Hokkaido
..... Y. Hariya...204

Communications on Minerals of Japan (Part 7).....Mumeikai Group...208

17. Thorite and Zircon from Ishikawa District, Fukushima Prefecture
..... K. Sakurai

18. Uranothorite from Kamiotomo, Iwate Prefecture .....
..... O. Nagashima and K. Sakurai

19. Allanite from Kamiotomo, Iwate Prefecture.....
.....K. Nagashima and K. Sakurai

Reviews

X-ray Diffractometer.....Y. Takano and Y. Iitaka...214

Proceedings 230

Printed by "HERALD" Printing Co., Ltd.